10. After 48 hours, the medium was replaced with a new medium containing mock VSVG-pp or HCVpp expressing luciferase. After another 48 hours, pseudoparticles entry was determined by measuring the luciferase activity. In order to compare the HCVpp entry between IPK17 and HuH7.5.1 cells, the luciferase expression from VSV-Gpp entry was used an internal control, while that from HCVpp was plotted relatively.
(TIF)

Acknowledgments

We want to thank Dr. Michinori Kohara (Tokyo Metropolitan Institute for Medical Science, Tokyo, Japan); Dr. Tadatsugu Taniguchi (University of Tokyo, Yokyo, Japan); Dr. Thomas Pietschmann (Division of Experimental Virology, TWINCORE, Hannover, Germany); and Dr. Makoto Hijikata (The Institute for Virus Research, Kyoto University, Japan) for their generous supply of research material. Dr. Hussein H. Aly was supported by a JSPS postdoctoral fellowship from the Japan Society for the Promotion of Science.

Author Contributions

Conceived and designed the experiments: HHA TS. Performed the experiments: HHA HO. Analyzed the data: HHA MM HO HS TS. Contributed reagents/materials/analysis tools: KS TW. Wrote the paper: HHA.

References

1. Seto WK, Lai CL, Fung J, Hung I, Yuen J, et al. (2010) Natural history of chronic hepatitis C: Genotype 1 versus genotype 6. J Hepatol.
2. Uprichard SL, Chung J, Chisari FV, Wakita T (2006) Replication of a hepatitis C virus replicon clone in mouse cells. Virol J 3: 89.
3. Ploss A, Evans MJ, Gaysinskaya VA, Panis M, You H, et al. (2009) Human occludin is a hepatitis C virus entry factor required for infection of mouse cells. Nature 457: 882–886.
4. Diamond MS (2009) Mechanisms of evasion of the type I interferon antiviral response by flaviviruses. J Interferon Cytokine Res 29: 521–530.
5. O'Neill LA, Bowie AG (2010) Sensing and signaling in antiviral innate immunity. Curr Biol 20: R328–333.
6. Platanias LC (2005) Mechanisms of type-I- and type-II-interferon-mediated signalling. Nat Rev Immunol 5: 375–386.
7. Tanaka Y, Nishida N, Sugiyama M, Kurosaki M, Matsuura K, et al. (2009) Genome-wide association of IL28B with response to pegylated interferon-alpha and ribavirin therapy for chronic hepatitis C. Nat Genet 41: 1105–1109.
8. Thompson AJ, Muir AJ, Sulkowski MS, Ge D, Fellay J, et al. (2010) Interleukin-28B polymorphism improves viral kinetics and is the strongest pretreatment predictor of sustained virologic response in genotype 1 hepatitis C virus. Gastroenterology 139: 120–129. e118.
9. Sumpter R, Jr., Loo YM, Foy E, Li K, Yoneyama M, et al. (2005) Regulating intracellular antiviral defense and permissiveness to hepatitis C virus RNA replication through a cellular RNA helicase, RIG-I. J Virol 79: 2689–2699.
10. Foy E, Li K, Sumpter R, Jr., Loo YM, Johnson CL, et al. (2005) Control of antiviral defenses through hepatitis C virus disruption of retinoic acid-inducible gene-I signaling. Proc Natl Acad Sci U S A 102: 2986–2991.
11. Oshiumi H, Ikeda M, Matsumoto M, Watanabe A, Takeuchi O, et al. (2010) Hepatitis C virus core protein abrogates the DDX3 function that enhances IPS-1-mediated IFN-beta induction. PLoS One 5: e14258.
12. Oshiumi H, Miyashita M, Inoue N, Okabe M, Matsumoto M, et al. (2010) The ubiquitin ligase Riplet is essential for RIG-I-dependent innate immune responses to RNA virus infection. Cell Host Microbe 8: 496–509.
13. Ishiyama T, Kano J, Minami Y, Iijima T, Morishita Y, et al. (2003) Expression of HNFs and C/EBP alpha is correlated with immunocytochemical differentiation of cell lines derived from human hepatocellular carcinomas, hepatoblastomas and immortalized hepatocytes. Cancer Sci 94: 757–763.
14. Berg CP, Schlosser SF, Neukirchen DK, Papadakis C, Gregor M, et al. (2009) Hepatitis C virus core protein induces apoptosis-like caspase independent cell death. Virol J 6: 213.
15. Deng L, Adachi T, Kitayama K, Bungyoku Y, Kitazawa S, et al. (2008) Hepatitis C virus infection induces apoptosis through a Bax-triggered, mitochondrion-mediated, caspase 3-dependent pathway. J Virol 82: 10375–10385.
16. Zhu H, Dong H, Eksioglu E, Hemming A, Cao M, et al. (2007) Hepatitis C virus triggers apoptosis of a newly developed hepatoma cell line through antiviral defense system. Gastroenterology 133: 1649–1659.
17. Ray RB, Meyer K, Ray R (1996) Suppression of apoptotic cell death by hepatitis C virus core protein. Virology 226: 176–182.
18. Mankouri J, Dallas ML, Hughes ME, Griffin SD, Macdonald A, et al. (2009) Suppression of a pro-apoptotic K+ channel as a mechanism for hepatitis C virus persistence. Proc Natl Acad Sci U S A 106: 15903–15908.
19. Ladu S, Calvisi DF, Conner EA, Farina M, Factor VM, et al. (2008) E2F1 inhibits c-Myc-driven apoptosis via PIK3CA/Akt/mTOR and COX-2 in a mouse model of human liver cancer. Gastroenterology 135: 1322–1332.
20. Lowe SW, Lin AW (2000) Apoptosis in cancer. Carcinogenesis 21: 485–495.
21. Schulze-Bergkamen H, Krammer PH (2004) Apoptosis in cancer–implications for therapy. Semin Oncol 31: 90–119.
22. Ebihara T, Shingai M, Matsumoto M, Wakita T, Seya T (2008) Hepatitis C virus-infected hepatocytes extrinsically modulate dendritic cell maturation to activate T cells and natural killer cells. Hepatology 48: 48–58.
23. Mateu G, Donis RO, Wakita T, Bukh J, Grakoui A (2008) Intragenotypic JFH1 based recombinant hepatitis C virus produces high levels of infectious particles but causes increased cell death. Virology 376: 397–407.
24. Bitzegeio J, Bankwitz D, Hueging K, Haid S, Brohm C, et al. (2010) Adaptation of hepatitis C virus to mouse CD81 permits infection of mouse cells in the absence of human entry factors. PLoS Pathog 6: e1000978.
25. Lin LT, Noyce RS, Pham TN, Wilson JA, Sisson GR, et al. (2010) Replication of subgenomic hepatitis C virus replicons in mouse fibroblasts is facilitated by deletion of interferon regulatory factor 3 and expression of liver-specific microRNA 122. J Virol 84: 9170–9180.
26. Ishigami A, Fujita T, Handa S, Shirasawa T, Koseki H, et al. (2002) Senescence marker protein-30 knockout mouse liver is highly susceptible to tumor necrosis factor-alpha- and Fas-mediated apoptosis. Am J Pathol 161: 1273–1281.
27. Akazawa T, Ebihara T, Okuno M, Okuda Y, Shingai M, et al. (2007) Antitumor NK activation induced by the Toll-like receptor 3-TICAM-1 (TRIF) pathway in myeloid dendritic cells. Proc Natl Acad Sci U S A 104: 252–257.
28. Ebihara T, Azuma M, Oshiumi H, Kasamatsu J, Iwabuchi K, et al. (2010) Identification of a polyI:C-inducible membrane protein that participates in dendritic cell-mediated natural killer cell activation. J Exp Med 207: 2675–2687.
29. Aly HH, Qi Y, Atsuzawa K, Usuda N, Takada Y, et al. (2009) Strain-dependent viral dynamics and virus-cell interactions in a novel in vitro system supporting the life cycle of blood-borne hepatitis C virus. Hepatology 50: 689–696.
30. Aly HH, Shimotohno K, Hijikata M (2009) 3D cultured immortalized human hepatocytes useful to develop drugs for blood-borne HCV. Biochem Biophys Res Commun 379: 330–334.
31. Wakita T, Pietschmann T, Kato T, Date T, Miyamoto M, et al. (2005) Production of infectious hepatitis C virus in tissue culture from a cloned viral genome. Nat Med 11: 791–796.
32. Aly HH, Watashi K, Hijikata M, Kaneko H, Takada Y, et al. (2007) Serum-derived hepatitis C virus infectivity in interferon regulatory factor-7-suppressed human primary hepatocytes. J Hepatol 46: 26–36.
33. Haid S, Windisch MP, Bartenschlager R, Pietschmann T (2010) Mouse-specific residues of claudin-1 limit hepatitis C virus genotype 2a infection in a human hepatocyte cell line. J Virol 84: 964–975.

Ann Surg Oncol (2012) 19:418–425
DOI 10.1245/s10434-011-1866-1

Annals of
SURGICAL ONCOLOGY
OFFICIAL JOURNAL OF THE SOCIETY OF SURGICAL ONCOLOGY

ORIGINAL ARTICLE – HEPATOBILIARY TUMORS

Impact of Pegylated Interferon Therapy on Outcomes of Patients with Hepatitis C Virus-Related Hepatocellular Carcinoma After Curative Hepatic Resection

Yoshisato Tanimoto, MD[1], Hirotaka Tashiro, MD[1], Hiroshi Aikata, MD[2], Hironobu Amano, MD[1], Akihiko Oshita, MD[1], Tsuyoshi Kobayashi, MD[1], Shintaro Kuroda, MD[1], Hirofumi Tazawa, MD[1], Shoichi Takahashi, MD[2], Toshiyuki Itamoto, MD[3], Kazuaki Chayama, MD[2], and Hideki Ohdan, MD[1]

[1]Department of Gastroenterological Surgery, Hiroshima University Hospital, Hiroshima, Japan; [2]Department of Gastroenterology, Hiroshima University Hospital, Hiroshima, Japan; [3]Department of Surgery, Prefectural Hiroshima Hospital, Hiroshima, Japan

ABSTRACT

Background. Several published reports investigating the effects of interferon (IFN) therapy on survival and tumor recurrence after curative resection of hepatocellular carcinoma (HCC) have been inconclusive. The aim of this study is to investigate the efficacy of pegylated-IFN (peg-IFN) therapy after curative hepatic resection for HCC in patients infected with hepatitis C virus (HCV).

Methods. Data from 175 patients who underwent curative hepatic resection for HCC associated with HCV were retrospectively collected and analyzed; 75 patients received peg-IFN therapy after surgery, whereas 100 patients did not receive IFN therapy. To overcome biases resulting from the different distribution of covariates in the two groups, a one-to-one match was created using propensity score analysis. After matching, patient outcomes were analyzed.

Results. After one-to-one matching, patients ($n = 38$) who received peg-IFN therapy after surgery and patients ($n = 38$) who did not receive IFN therapy had the same preoperative and operative characteristics. The 3- and 5-year overall survival rates of patients who received peg-IFN therapy after hepatic resection were significantly higher than those of patients who did not receive IFN therapy ($P = 0.00135$). The 3- and 5-year overall survival rates were 100 and 91.7% and 76.6 and 50.6% in the peg-IFN group and non-IFN group, respectively. There was no significant difference in disease-free survival between the two matched groups ($P = 0.886$).

Conclusion. Peg-IFN therapy may be effective as an adjuvant chemopreventive agent after hepatic resection in patients with HCV-related HCC.

First Received: 14 February 2011;
Published Online: 28 June 2011

H. Tashiro, MD
e-mail: htashiro@hiroshima-u.ac.jp

Hepatic resection is a well-accepted therapy for hepatocellular carcinoma (HCC), but many patients show cancer recurrence and the cumulative 5-year HCC recurrence rate exceeds 70%.[1–3] This high incidence of tumor recurrence after hepatic resection remains a major drawback. Some benefits of interferon (IFN) therapy on tumor recurrence and survival have been reported.[4–10] IFN suppresses replication of hepatitis C virus (HCV) and exerts a tumoricidal effect on a number of tumors, including HCC.[10,11] However, several randomized controlled trials (RCTs) have revealed inconclusive results regarding the effects of IFN on survival and tumor recurrence after curative resection or ablation of HCC, either because the effects were not statistically significant or because they were considered only with respect to defined subpopulations.[12–15]

Recently, combination therapy consisting of pegylated interferon (peg-IFN) plus ribavirin (RBV) has been developed, and the effect of this combination has been reported to be higher than that of conventional IFN therapy.[16,17] Peg-IFN has an extended serum half-life that provides viral suppression for 7 days, thus allowing weekly administration and enhanced clinical efficacy.[17] Most Japanese patients infected with HCV are infected with HCV genotype Ib and have high viral load. Moreover, treatment with conventional IFN is complicated by a low sustained viral response (SVR) rate of 20–30%.[18–20]

However, peg-IFN plus RBV combination therapy has good tolerability in Japanese patients with HCV and resulted in an SVR rate of approximately 40–50%.[21–23] The impact of adjuvant immunotherapy with IFN after curative resection of HCC is debatable, and few studies have investigated the effects of peg-IFN plus RBV combination therapy on survival and recurrence after curative resection of HCC.

In the present study, we aim to investigate the impact of peg-IFN plus RBV combination therapy on survival and HCC recurrence after curative resection in patients infected with HCV.

PATIENTS AND METHODS

Patients and HCV Diagnosis

From June 2003 to June 2009, 370 HCC patients underwent hepatectomy as initial treatment at the Department of Gastroenterological Surgery, Hiroshima University Hospital, Japan. Of the 370 patients, 175 patients who were HCV RNA-positive/hepatitis B surface antigen-negative underwent curative hepatectomy. Of the 175 patients, 75 patients received IFN therapy after hepatectomy, and 100 patients did not receive any IFN therapy. Of the 75 patients who received IFN, 20 patients who received IFNs such as IFN-α or IFN-β were excluded. Of the 55 patients who received peg-IFN therapy, 43 patients who started peg-IFN within 9 months after curative resection were enrolled in this analysis. Twenty-four patients who had early recurrence of HCC within 9 months after surgery were excluded from the 100 patients who did not receive any IFN therapy, because these patients could lose the opportunity to receive IFN therapy for HCC recurrence if these patients were assigned to the peg-IFN therapy. Consequently, 119 patients were eventually enrolled in this study. Of these 119 patients, 43 received peg-IFN therapy within 9 months after hepatectomy, and 76 did not receive any IFN therapy.

Curative hepatectomy was defined as removal of all recognizable tumors. HCV RNA levels were measured by quantitative reverse-transcription polymerase chain reaction (RT-PCR; Amplicor, Roche Diagnostic Systems, CA, USA). HCV genotype was determined by PCR using a mixed primer set derived from the nucleotide sequences of the NS5 region. HCV negativity was evaluated by quantitative RT-PCR. The lower limit of the assay was 5 kIU/ml (equivalent to 5,000 copies/ml) in the quantitative method and 50 IU/ml (equivalent to 50 copies/ml) in the qualitative method. SVR was defined as undetectable HCV RNA at 24 weeks after completion of IFN therapy. The study was approved by the concerned institutional review boards. Written informed consent was obtained from all patients.

Preoperative Diagnosis and Evaluation of HCC

Hepatocellular carcinoma was diagnosed on the basis of routine imaging modalities such as Doppler ultrasonography (US), computed tomography (CT) during hepatic angiography (CTHA) and CT during arterial portography (CTAP), and magnetic resonance imaging. Tumor stage, liver damage classification, and surgical procedures were defined according to the General Rules for Clinical and Pathologic Study of Primary Liver Cancer, fifth edition, by the Liver Cancer Study Group of Japan.[24]

Hepatectomy

The surgical procedure was determined according to tumor extent and hepatic reserve function. Liver function was assessed by liver damage classification, Child–Pugh classification, and indocyanine green retention rate at 15 min (ICGR 15).[25,26] If permitted by liver function, anatomic resection was performed.[27,28] In patients with insufficient hepatic reserve, limited resection was performed. We divided the liver parenchyma by using an ultrasonic dissector.[29] Postoperative complications were graded according to the method described by Clavien et al.[30]

Follow-Up

Follow-up evaluation after the surgery consisted of monthly blood chemistry tests and measurements of levels of tumor markers, including alpha-fetoprotein and des-gamma-carboxy prothrombin. Patients were examined by US every 3 months and by CT every 6 months. When recurrence was indicated by any of these examinations, patients were examined by CTAP and CTHA.

Patient Selection for IFN Therapy

Patients with HCV genotype 1b in the IFN group received peg-IFNα-2b (Pegintron; Schering-Plough, NJ, USA) at weekly dosage of 1.5 μg/kg subcutaneously for 48 weeks. Daily RBV (Rebetrol, Schering-Plough) was administered orally for 48 weeks, and the dosage was adjusted according to weight (600 mg for patients weighing $\leq$60 kg, 800 mg for those weighing 60–80 kg). Patients with HCV genotype 2 received IFN monotherapy for 24 weeks. Blood samples were obtained every 4 weeks and analyzed for HCV RNA levels. All patients were informed about IFN therapy after hepatectomy, and only consenting patients received IFN therapy. The eligibility criteria for IFN therapy were as follows: (1) detectable serum HCV RNA level, (2) Eastern Cooperative Oncology

Group (ECOG) performance score of 0 or 1, (3) platelet count ≥70,000/μl, (4) patients with no uncompensated cirrhosis (Child class C), and (5) hemoglobin concentration ≥10 g/dl. Peg-IFN therapy was commenced within 24 weeks of surgery or after the eligibility criteria were fulfilled.

Safety Assessments and Dose Modification of Peg-IFN Therapy

Adverse events were graded as mild, moderate, severe, or potentially life-threatening according to a modified World Health Organization grading system. The dose of peg-IFN was decreased by 50% and that of RBV was lowered to half in case of severe adverse events or when laboratory results revealed any of the following: hemoglobin concentration <10 g/dl in patients with no cardiac disease, decrease in hemoglobin concentration >2 g/dl in patients with cardiac disease, white blood cell count <3,000/mm^3, or platelet count <50,000/mm^3. Full dosage could be resumed on resolution of the adverse events. Treatment was permanently discontinued in case of life-threatening events or when laboratory results revealed hemoglobin concentration <7.5 g/dl after 4 weeks of dose reduction, white blood cell count <1,500/mm^3, or platelet count <30,000 mm^3.

Treatment for Recurrence

Patients with intrahepatic HCC recurrence were managed with ablative therapies such as radiofrequency ablation (RFA), percutaneous ethanol injection therapy, transarterial chemoembolization, or surgery including living-donor liver transplantation according to the tumor characteristics (number, size, and location of the tumors) and liver function.

Statistical Analyses

Categorical variables were compared using the chi-square test, and continuous variables were compared using the Mann–Whitney *U*-test. Overall survival and disease-free survival analyses were performed using Kaplan–Meier methods; comparisons between different groups were performed using the log-rank test. *P* value of less than 0.05 was considered significant. Calculations were performed using SPSS software (version 16; SPSS Inc., IL, USA).

Propensity analysis was performed using logistic regression to create a propensity score for the IFN and non-IFN therapy groups.[31,32] Variables entered in the propensity model were age, sex, HCV genotype, liver function test, tumor factors, and operative factors. The model was then used to provide a one-to-one match between the two groups by using the nearest-neighbor matching method.[33,34] Survival and disease-free survival analyses were performed in each matched subgroup to assess the impact of peg-IFN therapy on mortality after adjusting for the confounding factors.

RESULTS

Characteristics and Postoperative Course of the Entire Population

Differences in the characteristics of patients who received peg-IFN therapy after hepatic resection and those who did not receive IFN therapy after hepatic resection are presented in Table 1. Patients who received peg-IFN therapy were younger (65 vs. 71 years; $P = 0.0003$). Regarding tumor characteristics, there was no significant difference between the two groups. Operation times tended to be longer in patients who received peg-IFN therapy than in those who did not receive IFN therapy (260 vs. 242 min; $P = 0.05$). There were no hospital-related deaths in this study. Postoperative complications did not differ between the two groups. In the entire population, the 3- and 5-year overall survival rates of patients who received peg-IFN therapy after hepatic resection were significantly higher than those of patients who did not receive IFN therapy ($P = 0.0024$) (Fig. 1a). However, there was no significant difference in disease-free survival between the two groups ($P = 0.795$) (Fig. 1b).

Results After Propensity Score Matching

Characteristics of the patients after propensity score analysis are presented in Table 1. Thirty-eight of the 43 patients who received peg-IFN therapy after hepatic resection and an equal number of the 76 patients who did not receive IFN therapy were matched after covariate adjustment. The study group of 76 patients was well matched; in particular, all covariates that significantly affected recurrence and postoperative liver failure in the entire study group were equally distributed between the two matched groups. Matched patients who received peg-IFN therapy after hepatic resection had similar total bilirubin and serum albumin levels and similar platelet counts to matched patients who did not receive IFN therapy. Similarly, the tumor characteristics, the surgical procedure, operation times, and blood loss during the operation in matched patients who received peg-IFN therapy were almost similar to those in patients who did not receive IFN therapy. There were no hospital-related deaths in the matched groups. Postoperative complications also did not differ between the two groups. The median follow-up period for patients who received peg-IFN and those who

TABLE 1 Baseline characteristics and operative data on patients who underwent hepatectomy: data are reported for whole study and for the matched study population after propensity score analysis

	Overall series		*P* value	Propensity-matched series		*P* value
	IFN (+) $n = 43$	IFN (−) $n = 76$		Peg-IFN (+) $n = 38$	IFN (−) $n = 38$	
Age (years)	65 (53–78)	71 (48–83)	0.0003	65.5 (53–75)	69 (51–80)	0.2
Sex (male/female)	27/16	47/29	0.918	23/15	25/13	0.634
Preoperative IFN	24 (55.8%)	29 (38.1%)	0.06	20 (52.6%)	14 (36.8%)	0.16
HCV genotype			0.876			0.6
1b	34	61		29	27	
2b	9	15		9	11	
Diabetes mellitus	11 (25.6%)	22 (28.9%)	0.856	11 (28.9%)	13 (34.2%)	0.621
ECOG PS			0.831			0.644
0	39	68		36	35	
1	4	8		2	3	
Platelet (104/mm^3)	10.3 (3.3–26.6)	10.3 (3.8–40.3)	0.381	9.75 (3.3–21.5)	11.2 (3.8–40.3)	0.454
T-Bil (mg/dl)	0.7 (0.3–1.4)	0.8 (0.3–1.7)	0.292	0.7 (0.4–1.4)	0.7 (0.3–1.7)	0.798
AST (IU/l)	42 (18–121)	48 (16–150)	0.152	43.5 (18–127)	41.5 (6–150)	0.567
ALT (IU/l)	38 (13–127)	41.5 (10–196)	0.987	40.5 (11–127)	37.5 (10–196)	0.226
Albumin (g/dl)	3.8 (2.8–5.2)	3.8 (2.5–4.9)	0.215	3.8 (2.8–5.2)	3.8 (2.5–4.5)	0.469
ICGR 15 (%)	17.9 (7.4–77.4)	18.7 (4.6–50.5)	0.734	17.65 (7.4–40.0)	17.55 (4.6–40.0)	0.561
AFP (ng/ml)	11.6 (0.5–3405)	27.6 (0.5–36572)	0.176	13.95 (0.5–3405)	22.9 (0.5–513)	0.635
Child–Pugh grade			0.665			0.556
A	41 (95.3%)	69 (90.8%)		37 (97.4%)	36 (94.7%)	
B	2 (4.7%)	7 (9.2%)		1 (2.6%)	2 (5.3%)	
Hepatic resection			0.322			0.373
Hr0	20 (46.5%)	49 (64.5%)		18 (47.4%)	23 (60.5%)	
HrS	13 (30.2%)	18 (23.7%)		12 (31.6%)	9 (23.7%)	
Hr1	3 (7.0%)	4 (5.3%)		2 (5.3%)	3 (7.9%)	
Hr2	7 (16.3%)	5 (6.6%)		6 (15.8%)	2 (5.3%)	
Hr3	0 (0%)	0 (0%)		0 (0%)	0 (0%)	
Operation time (min)	260 (128–623)	242 (90–580)	0.0514	257 (128–623)	247.5 (90–580)	0.18
Blood loss (ml)	200 (20–1900)	225 (10–960)	0.996	210 (20–1900)	210 (10–960)	0.803
Postoperative complications			0.933			0.798
IIIa	4	6		2	2	
IIIb	1	1		1	1	
IVa	1	1		1	0	
Stage			0.315			0.293
I	14 (32.6%)	19 (25.0%)		13 (34.2%)	9 (23.7%)	
II	18 (41.9%)	44 (57.9%)		15 (39.5%)	23 (60.5%)	
III	9 (20.9%)	12 (15.8%)		9 (23.7%)	6 (15.8%)	
IV-A	2 (4.7%)	1 (1.3%)		1 (2.6%)	0 (0.0%)	
Single tumor	28 (65.1%)	57 (75.0%)	0.252	25 (65.8%)	29 (76.3%)	0.312
Tumor size			0.712			0.589
≥3 cm	15 (34.9%)	24 (31.6%)		10 (26.3%)	8 (21.1%)	
<3 cm	28 (65.1%)	52 (68.4%)		28 (73.7%)	30 (78.9%)	
Vascular invasion	4 (9.3%)	3 (3.9%)	0.233	3 (7.9%)	0 (0.0%)	0.239

Continuous variables expressed as median (range)

Hepatic resection and stage were according to General Rules for the Clinical and pathological Study of Primary Liver Cancer, by Liver cancer Study Group of Japan, 5th edition, Kanehara Co., Ltd

Hr0: limited resection, HrS: segmentectomy, Hr1: sectionectomy, Hr2: hemihepatectomy, Hr3: more than hemihepatectomy

T-Bil total bilirubin, *PS* performance status, *AST* aspartate aminotransferase, *ALT* alanine aminotransferase, *ICGR 15* indocyanine green retention rate at 15 min, *AFP* alpha-fetoprotein,

did not receive IFN therapy was 3.8 (1.2–6.9) and 3.5 (1.3–6.8) years, respectively. In the matched study groups, the 3- and 5-year overall survival rates of patients who received peg-IFN therapy after hepatic resection were significantly higher than those of patients who did not receive IFN therapy ($P = 0.00135$) (Fig. 1c). However, there was no significant difference in disease-free survival between the two matched groups ($P = 0.886$) (Fig. 1d).

In the matched 38 patients of the peg-IFN group, peg-IFN therapy was initiated at a median of 4.3 (0.9–9.6) months after hepatic resection. Thirty-one of 38 HCC patients began peg-IFN therapy within 6 months after hepatectomy. Seven patients required more than 6 months to commence peg-IFN therapy. Two patients required a longer time to recover platelet counts of more than 70,000/μl. Five patients required a longer time to decide to receive peg-IFN therapy. Sixteen (42.1%) of the matched 38 patients who received peg-IFN therapy after hepatectomy attained SVR. Among 16 patients who attained SVR, 10 patients received full-dose peg-IFN therapy without dose reduction, whereas 6 patients received a reduced dose of peg-IFN and/or RBV until completion of treatment. Nine patients discontinued peg-IFN therapy because of adverse events such as thrombocytopenia and neutropenia ($n = 2$), skin eruption ($n = 1$), depression ($n = 2$), and severe malaise ($n = 4$). Three patients discontinued peg-IFN therapy because of HCC recurrence. Adherence to peg-IFN therapy was 68.4% in this study. No life-threatening adverse events were observed, and none of the total 15 deaths in both sets of matched patients were related to the IFN treatment or to surgical procedures. The 3- and 5-year overall survival rates of patients ($n = 16$) who attained SVR after peg-IFN therapy were 100% and 100%, respectively; those of patients who did not attain SVR ($n = 22$) were 100 and 85.7%, respectively; and those of patients who did not receive IFN therapy were 76.6 and 50.6%, respectively. There was a statistically significant difference in overall survival among the three groups ($P = 0.005$) (Fig. 2a). However, there was no statistically significant difference in disease-free survival among the three groups ($P = 0.90$) (Fig. 2b).

Table 2 presents the patterns of cancer recurrence and the treatment details of the recurrences in both groups. Twenty-one (55.3%) of the patients who received peg-IFN therapy after hepatic resection and 17 (44.7%) of the patients who did not receive IFN therapy had HCC recurrences after hepatic resection. Regarding the pattern of recurrence, the proportion of patients who had multiple

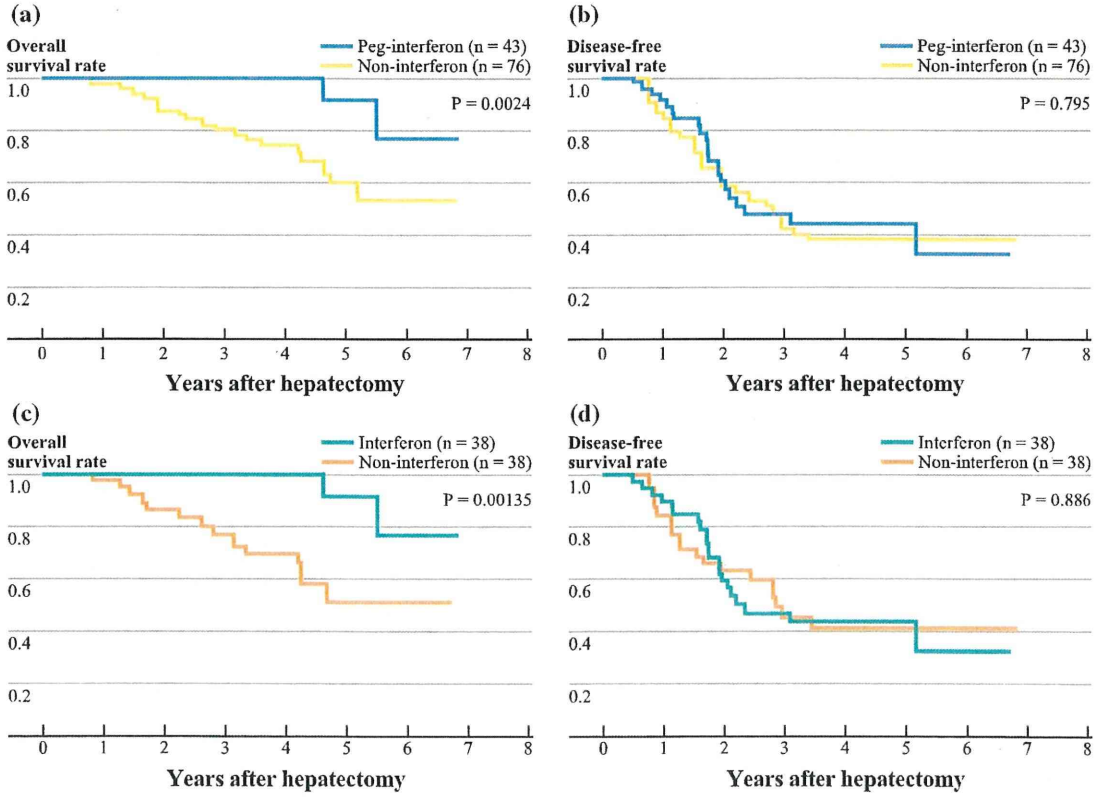

FIG. 1 Overall survival (**a**) and disease-free survival (**b**) of the entire study population of 175 patients with hepatitis C-related HCC with respect to IFN therapy after hepatic resection. Overall survival (**c**) and disease-free (**d**) survival of the matched study population of 76 patients with hepatitis C-related HCC with respect to IFN therapy after hepatic resection

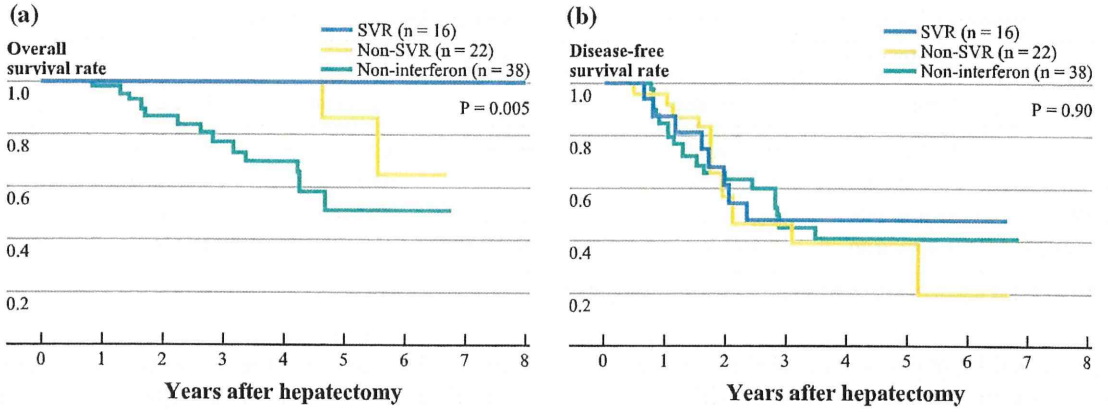

FIG. 2 Overall survival and disease-free survival of patients with hepatitis C-related HCC with respect to SVR after IFN therapy

intrahepatic recurrences (more than four nodules) was significantly lower in the peg-IFN group than in the non-IFN group ($P = 0.0047$). The proportion of patients in whom surgery or RFA was selected for treatment was significantly higher in the peg-IFN group than in the non-IFN group ($P = 0.0346$). Furthermore, regarding re-recurrence of HCC after treatment of the first-recurrent HCC, the 1-year disease-free survival rates of patients after treatment of the first-recurrent HCC was 48.5% in patients ($n = 21$) who received peg-IFN therapy and 12.5% in patients ($n = 17$) who did not receive IFN therapy. There was a statistically significant difference in disease-free survival between the two groups ($P = 0.0012$) (Fig. 3).

A comparison of results of the preoperative liver function test with those of postoperative 1-year liver function tests is presented in Table 3. In patients who received peg-IFN therapy, total bilirubin levels 1 year after surgery were significantly decreased compared with preoperative total bilirubin levels ($P = 0.018$), whereas in patients who did not receive IFN therapy, the total bilirubin level at 1 year after surgery was similar to the total bilirubin level before surgery ($P = 0.107$).

TABLE 2 Recurrence and treatments for recurrence after hepatic resection

	Peg-IFN (+) ($n = 38$)	IFN (−) ($n = 38$)	*P* value
HCC recurrence[a]: yes	21 (55.3%)	17 (44.7%)	0.359
Pattern of recurrence[b]			0.0047
Intrahepatic (single)	9 (42.9%)	8 (47.1%)	
Intrahepatic (2–3)	10 (47.6%)	1 (5.9%)	
Intrahepatic (multiple)	2 (9.5%)	8 (47.1%)	
Main modalities[b]			0.0346
Repeat hepatectomy	8 (38.1%)	2 (11.8%)	
RFA	8 (38.1%)	4 (23.5%)	
TACE	5 (23.8%)	11 (64.7%)	

peg-IFN pegylated interferon, *RFA* radiofrequency ablation, *TACE* transcatheter arterial chemoembolization

[a] Data expressed as number of patients (percentage of total patients)

[b] Data expressed as number of patients (percentage of patients who had a recurrence)

DISCUSSION

Our results revealed that peg-IFN therapy after hepatic resection improved the outcomes of HCV patients, although the interval of disease-free survival was not prolonged. Peg-IFN therapy after hepatectomy improved hepatic reserve function and suppressed multiple HCC recurrences (more than four nodules). Furthermore, re-recurrence after treatment of first-recurrent HCC after hepatic resection was significantly suppressed in the peg-IFN group compared with that in the non-IFN group. IFN has been reported to exert antitumor effects. IFN increases natural killer cell activity and exhibits antiangiogenic properties.[35,36] IFN has also been reported to be effective in eradicating HCV RNA

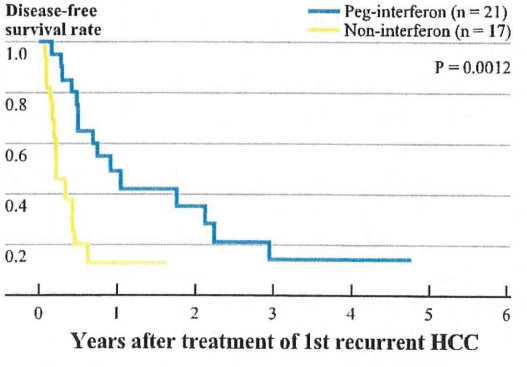

FIG. 3 Comparison of disease-free survival rate after treatment of first-recurrent HCC in patients who received peg-IFN therapy or in those who did not receive IFN therapy

TABLE 3 Comparison of preoperative liver function with 1-year liver function after hepatic resection

	Peg-IFN (+)		*P* value	IFN (−)		*P* value
	Preoperative	1 Year after surgery		Preoperative	1 Year after surgery	
T-Bil (mg/dl)	0.82 ± 0.29	0.71 ± 0.26	0.0189	0.81 ± 0.32	0.92 ± 0.35	0.107
AST (IU/l)	50.1 ± 24.1	45.8 ± 23.5	0.310	42.1 ± 18.9	56.1 ± 26.7	0.0110
ALT (IU/l)	51.3 ± 28.6	36.4 ± 22.8	0.00809	40.3 ± 24.3	49.7 ± 25.8	0.0918
Albumin (g/dl)	3.89 ± 0.80	3.99 ± 0.71	0.251	3.73 ± 0.45	3.75 ± 0.44	0.807

peg-IFN pegylated interferon, *AST* aspartate aminotransferase, *ALT* alanine aminotransferase

from serum and hepatic tissue, thereby preventing deterioration of liver function in patients with HCV infection.[37] IFN prevents worsening of compensated cirrhosis.[18,37] Our results are compatible with those reported in those studies. In the peg-IFN group, most patients with HCC recurrence could undergo curative treatments such as repeat hepatectomy or RFA as a recurrence treatment, because the number of recurrent tumors was usually limited to three. IFN therapy appears to increase survival not only by improving residual liver function and increasing the possibility of radical treatment of recurrences but also by suppressing re-recurrence after the first recurrence of HCC.

The current study also revealed that the overall survival of patients with SVR was significantly better than that of patients without SVR. This result suggests that IFN prolongs the outcomes of patients with HCC after hepatic resection by causing remission of active hepatitis and eradication of HCV RNA in patients who attained SVR after hepatic resection.

In this study, to clarify the impact of peg-IFN therapy on outcomes of HCV-related HCC after hepatic resection, patients who received IFNs such as IFN-α or IFN-β were excluded. RCTs investigating adjuvant effects of IFN after resection or ablation of HCC were performed using IFN-α. Few studies have investigated the effects of peg-IFN plus RBV combination therapy on survival and recurrence after curative resection of HCC. Combination therapy with peg-IFN and RBV has recently been developed, and peg-IFN therapy has resulted in significantly higher SVR rates and better tolerability than treatment with IFN-α.[21,23] In our study, incidence of SVR after hepatic resection was 42.1%, which was higher than that in previous studies that reported an SVR rate of 0–10%.[12–14] The compliance of patients to peg-IFN therapy observed in the present study (68.4%) was higher than that reported elsewhere (approximately 40%).[14] This enhanced efficacy of the peg-IFN formulations might contribute to the prolonged survival of HCC patients after hepatic resection.

In this study, HCC patients who received peg-IFN therapy within 9 months after surgery were enrolled, and HCC patients who experienced recurrence of HCC within 9 months after hepatic resection were excluded from the non-IFN group, because these patients could lose the opportunity to receive IFN therapy for HCC recurrence on being assigned to the peg-IFN therapy group.

Before matching by using the propensity score, the clinical characteristics of the entire study population that can strongly influence outcomes differed significantly between the peg-IFN group and non-IFN group. The proportion of older patients was higher in the non-IFN group than in the peg-IFN group, whereas the proportion of patients who had longer operation times tended to be lower in the non-IFN group than in the peg-IFN group. To overcome bias due to the different distribution of the severity of liver function impairment between the two groups, a one-to-one match was created using propensity score analysis. After matching by propensity score, prognostic variables were appropriately handled, and there was no significant difference in prognostic factors between the two matched groups. This study had a limitation related to the small sample size after propensity score matching. To overcome this, further examination with larger sample sizes is necessary, and the potential efficacy of peg-IFN therapy must be validated in larger prospective RCTs.

CONCLUSIONS

Several previous RCTs investigating the effects of IFN on survival and tumor recurrence after hepatic resection were inconclusive. However, in the current study, peg-IFN therapy following hepatic resection improved the survival rates of hepatectomized patients with HCV-related HCC. The results of this study suggest that peg-IFN therapy is effective as an adjuvant chemopreventive agent after hepatic resection in patients with HCV-related HCC.

ACKNOWLEDGMENT The authors thank Prof. Junko Tanaka of the Department of Epidemiology, Infectious Disease Control and Prevention, Hiroshima University, for assistance in performing the propensity score analysis.

CONFLICT OF INTEREST The authors have no commercial associations (e.g., consultancies, stock ownership, equity interest, patent/licensing arrangements) that might pose a conflict of interest related to the submitted manuscript.

REFERENCES

1. Poon RTP, Fan ST, Lo CM, Liu CL, Wong J. Intrahepatic recurrence after curative resection of hepatocellular carcinoma: long-term results of treatment and prognostic factors. *Ann Surg.* 1999;229:216–22.
2. Minagawa M, Makuuchi M, Takayama T, Kokudo N. Selection criteria for repeat hepatectomy in patients with recurrent hepatocellular carcinoma. *Ann Surg.* 2003;238:703–10.
3. Itamoto T, Nakahara H, Amano H, et al. Repeat hepatectomy for recurrent hepatocellular carcinoma. *Surgery.* 2007;141:589–97.
4. Ikeda K, Saitoh S, Arase Y, Chayama K, et al. Effects of interferon therapy on hepatocellular carcinogenesis in patients with chronic hepatitis type C: a long-term observation study of 1,643 patients using statistical bias correction with proportional hazard analysis. *Hepatology.* 1999;29:1124–30.
5. Imai Y, Kawata S, Tamura S, et al. Relation of interferon therapy and hepatocellular carcinoma in patients with chronic hepatitis C. Osaka Hepatocellular Carcinoma Prevention Study Group. *Ann Intern Med.* 1998;129:94–9.
6. Camma C, Giunta M, Andreone P, Craxì A. Interferon and prevention of hepatocellular carcinoma in viral cirrhosis: an evidence-based approach. *J Hepatol.* 2001;34:593–602.
7. Nishiguchi S, Shiomi S, Nakatani S, et al. Prevention of hepatocellular carcinoma in patients with chronic active hepatitis C and cirrhosis. *Lancet.* 2001;357:196–7.
8. Tomimaru Y, Nagano H, Eguchi H, et al. Effects of preceding interferon therapy on outcome after surgery for hepatitis C virus-related hepatocellular carcinoma. *J Surg Oncol.* 2010;102: 308–14.
9. Jeong SC, Aikata H, Katamura Y, et al. Low-dose intermittent interferon-alpha therapy for HCV-related liver cirrhosis after curative treatment of hepatocellular carcinoma. *World J Gastroenterol.* 2007;13:5188–95.
10. Jeong SC, Aikata H, Kayamura Y, et al. Effects of a 24-week course of interferon-α therapy after curative treatment of hepatitis C virus-associated hepatocellular carcinoma. *World J Gastroenterol.* 2007;13:5343–50.
11. Harada H, Kitagawa M, Tanaka N, et al. Anti-oncogenic and oncogenic potentials of interferon regulatory factors-1 and -2. *Science.* 1993;259:971–4.
12. Liedtke C, Grogner N, Manns MP, Trautwein C. Interferon-alpha enhances TRAIL-mediated apoptosis by up-regulating caspase-8 transcription in human hepatoma cells. *J Hepatol.* 2006;44: 342–9.
13. Kubo S, Nishiguchi S, Hirohashi K, Tanaka H, Shuto T, Kinoshita H. Randomized clinical trial of long-term outcome after resection of hepatitis C virus-related hepatocellular carcinoma by postoperative interferon therapy. *Br J Surg.* 2002;89:418–22.
14. Ikeda K, Arase Y, Saitoh S, et al. Interferon beta prevents recurrence of hepatocellular carcinoma after complete resection or ablation of primary tumor-a prospective randomized study of hepatitis C virus-related liver cancer. *Hepatology.* 2000;32: 228–32.
15. Mazzaferro V, Romito R, Schiavo M, et al. Prevention of hepatocellular carcinoma recurrence with alpha-interferon after liver resection in HCV cirrhosis. *Hepatology.* 2006;44:1543–54.
16. Lo CM, Liu CL, Chan SC, et al. A randomized, controlled trial of postoperative adjuvant interferon therapy after resection of hepatocellular carcinoma. *Ann Surg.* 2007;245:831–42.
17. Manns MP, McHutchison JG, Gordon SC, et al. Peginterferon alfa-2b plus ribavirin compared with interferon alfa-2b plus ribavirin for initial treatment of chronic hepatitis C: a randomized trial. *Lancet.* 2001;358:958–65.
18. Fried MW, Shiffman ML, Rajender Reddy K, et al. Peginterferon alfa-2a plus ribavirin for chronic hepatitis C virus infection. *N Engl J Med.* 2002;347:975–82.
19. Yoshida H, Arakawa Y, Sata M, et al. Interferon therapy prolonged life expectancy among chronic hepatitis C patients. *Gastroenterology.* 2002;123:483–91.
20. Kiyosawa K, Uemura T, Ichijo T, et al. Hepatocellular carcinoma: recent trends in Japan. *Gastroenterology.* 2004;127: S17–26.
21. McHutchison JG, Gordon SC, Schiff ER, et al. Interferon alfa-2b alone or in combination with ribavirin as initial treatment for chronic hepatitis C. Hepatitis Interventional Therapy Group. *N Engl J Med.* 1998;339:1485–92.
22. Muir AJ, Bornstein JD, Killenberg PG. Peginterferon alfa-2b and ribavirin for the treatment of chronic hepatitis C in blacks and non-Hispanic whites. *N Eng J Med.* 2004;350:2265–71.
23. Shirakawa H, Matsumoto A, Joshita S, et al. Pretreatment prediction of virological response to peginterferon plus ribavirin therapy in chronic hepatitis c patients using viral and host factors. *Hepatology.* 2008;48:1753–60.
24. Kogure T, Ueno Y, Fukushima K, et al. Pegylated interferon plus ribavirin for genotype 1b chronic hepatitis C in Japan. *World J Gastroentrol.* 2008;14:7225–30.
25. Liver Cancer Study Group of Japan. General Rules for the Clinical and Pathological Study of Primary Liver Cancer. 5th ed. Tokyo: Kanehara; 2008.
26. Itamoto T, Nakahara H, Tashiro H, et al. Indications of partial hepatectomy for transplantable hepatocellular carcinoma with compensated cirrhosis. *Am J Surg.* 2005;189:167–72.
27. Oishi K, Itamoto T, Kobayashi T, et al. Hepatectomy for hepatocellular carcinoma in elderly patients aged 75 years or more. *J Gastrointest Surg.* 2009;13:695–701.
28. Makuuchi M, Hasegawa H, Yamazaki S. Ultrasonically guided subsegmentectomy. *Surg Gynecol Obstet.* 1985;161:346–50.
29. Yamamoto M, Takasaki K, Otsubo T, et al. Favorable surgical outcomes in patients with early hepatocellular carcinoma. *Ann Surg.* 2004;239:395–9.
30. Itamoto T, Katayama K, Nakahara H, Tashiro H, Asahara T. Autologous blood storage before hepatectomy for hepatocellular carcinoma with underlying liver disease. *Br J Surg.* 2003;90: 23–8.
31. Clavien PA, Barkun J, de Oliveira ML, et al. The Clavien–Dindo classification of surgical complications: five-year experience. *Ann Surg.* 2009;250:187–96.
32. Zinsmeister AR, Connor JT. Ten common statistical errors and how to avoid them. *Am J Gastroenterol.* 2008;103:262–6.
33. Rosenbaum PR, Rubin DB. The central role of the propensity score in observational studies for causal effects. *Biometrika.* 1983;70:41–55.
34. Rubin DB. Estimating causal effects from large data sets using propensity scores. *Ann Intern Med.* 1997;127:757–63.
35. D'Agostino RB Jr. Propensity score methods for bias reduction in the comparison of a treatment to non-randomized control group. *Stat Med.* 1998;17:2265–81.
36. Brinkmann V, Geiger T, Alkan S, Heusser CH. Interferon alpha increases the frequency of interferon gamma-producing human CD4+T cells. *J Exp Med.* 1993;178:1655–63.
37. Wang L, Tang ZY, Qin LX, et al. High-dose and long-term therapy with interferon-alfa inhibits tumor growth and recurrence in nude mice bearing human hepatocellular carcinoma xenografts with high metastatic potential. *Hepatology.* 2000;32:43–8.
38. Shiratori Y, Shiina S, Teratani T, et al. Interferon therapy after tumor ablation improves prognosis in patients with hepatocellular carcinoma associated with hepatitis C. *Ann Intern Med.* 2003;138: 299–306.

Research Article

EASL EUROPEAN ASSOCIATION FOR THE STUDY OF THE LIVER | JOURNAL OF HEPATOLOGY

Rho inhibitor prevents ischemia–reperfusion injury in rat steatotic liver

Shintaro Kuroda, Hirotaka Tashiro*, Yuka Igarashi, Yoshisato Tanimoto, Junko Nambu, Akihiko Oshita, Tsuyoshi Kobayashi, Hironobu Amano, Yuka Tanaka, Hideki Ohdan

Department of Surgery, Division of Frontier Medical Science, Programs for Biomedical Research, Graduate School of Biomedical Sciences, Hiroshima University, Hiroshima, Japan

Background & Aims: Hepatic stellate cells are thought to play a role in modulating intrahepatic vascular resistance based on their capacity to contract via Rho signaling. We investigated the effect of a Rho-kinase inhibitor on ischemia–reperfusion injury in the steatotic liver.

Methods: Steatotic livers, induced by a choline-deficient diet in rats, were subjected to ischemia–reperfusion injury. Hepatic stellate cells isolated from steatotic livers were analyzed for contractility and Rho signaling activity. The portal pressure of the perfused rat liver and the survival rate after ischemia–reperfusion were also investigated.

Results: Hepatic stellate cells from steatotic livers showed increased contractility and upregulation of Rho-kinase 2 compared with those from normal livers. Furthermore, endothelin-1 significantly enhanced the contractility and phosphorylation level of myosin light chain and cofilin in hepatic stellate cells isolated from steatotic livers. A specific Rho-kinase inhibitor, fasudil, significantly suppressed the contractility and decreased the phosphorylation levels of myosin light chain and cofilin. Serum levels of endothelin-1 were markedly increased after IR in rats with steatotic livers, whereas fasudil significantly decreased endothelin-1 serum levels. Rats with steatotic livers showed a significant increase in portal perfusion pressure after ischemia–reperfusion and a significant decrease in survival rate; fasudil treatment significantly reduced these effects.

Conclusions: Activation of Rho/Rho-kinase signaling in hepatic stellate cells isolated from steatotic livers is associated with an increased susceptibility to ischemia–reperfusion injury. A Rho-kinase inhibitor attenuated the activation of hepatic stellate cells isolated from steatotic livers and improved ischemia–reperfusion injury in steatotic rats.

Keywords: Steatosis; Ischemia–reperfusion injury; Hepatic stellate cell; Rho-kinase; Fasudil.

Received 19 November 2010; received in revised form 7 April 2011; accepted 29 April 2011; available online 12 July 2011

* Corresponding author. Address: Department of Surgery, Division of Frontier Medical Science, Programs for Biomedical Research, Graduate School of Biomedical Sciences, Hiroshima University, 1-2-3 Kasumi, Hiroshima 734-8551, Japan. Tel.: +81 82 257 5222; fax: +81 82 257 5224.

E-mail address: htashiro@hiroshima-u.ac.jp (H. Tashiro).

Abbreviations: IR, ischemia–reperfusion; SL, steatotic liver; HSCs, hepatic stellate cells; ROCK, Rho-kinase; MLC, myosin light chain; P-MLC, phosphorylated myosin light chain; NL, normal liver; fasudil, fasudil hydrochloride hydrate; NO, nitric oxide; L-NAME, *N*-nitro-L-arginine methyl ester; ET-1, endothelin-1; P-Cofilin, phosphorylated cofilin; AST, aspartate aminotransferase; ALT, alanine aminotransferase; H&E, hematoxylin and eosin; TUNEL, TdT-mediated dUTP-digoxigenin nick-end labeling; HSCs-SL, hepatic stellate cells isolated from rat steatotic liver; HSCs-NL, hepatic stellate cells isolated from rat normal liver; SECs, sinusoidal endothelial cells.

Introduction

Liver steatosis increases the risk of postoperative morbidity and mortality after liver surgery including liver transplantation [1–3]. Ischemia–reperfusion (IR) injury is one of the most critical complications commonly associated with liver surgery [4–6]. Although it is known that steatotic liver (SL) is particularly vulnerable to IR injury, the mechanisms underlying this increased susceptibility have not yet been clarified.

Experimental studies have indicated that the degree of steatosis is correlated with hepatic microcirculatory disturbances [4,5]. Fat droplet accumulation in the cytoplasm of hepatocytes is associated with an increase in cell volume, which may result in the partial or complete obstruction of the hepatic sinusoidal space and the reduction of sinusoidal blood flow. A continuous state of chronic cellular hypoxia persists in fatty hepatocytes, predisposing the SL to IR injury [7]. The sinusoidal lumens are narrowed by fibrin microthrombi and cellular debris during reperfusion, further decreasing sinusoidal perfusion.

Hepatic stellate cells (HSCs) play an important role in the regulation of hepatic microcirculation. HSCs undergo contraction or relaxation in response to certain stimuli and, as a result, regulate microcirculation by increasing or decreasing the diameter of the sinusoidal lumen [8]. HSCs also play an important role in IR injury [9]. Because HSCs are oxygen-sensing cells [10], they are likely to be activated by exposure to IR-induced oxidative stress, resulting in the disruption of hepatic microcirculation.

The Rho family of small GTPases is known to regulate cell shape and motility through reorganization of the actin cytoskeleton [11]. One of the putative Rho target proteins, the serine/threonine kinase ROCK, mediates cytoskeleton-dependent cell functions by enhancing the phosphorylation of myosin light

chain (MLC) [12]. An increase in phosphorylated MLC (P-MLC) increases the contractility of actomyosin and causes smooth muscle contraction [13]. In addition, P-MLC facilitates the clustering of integrins and the bundling of actin fibers [14], resulting in stimulus-induced cell adhesion and motility.

The contraction of HSCs narrows the sinusoidal lumen and reduces hepatic microcirculatory flow via Rho signaling. We reported previously that the Rho/ROCK signaling pathway played an important role in the activation of HSCs and that a ROCK inhibitor attenuated hepatic injury after warm IR and orthotopic liver transplantation in a rat model [9]. Recently, HSC activation has been shown to be correlated with the severity of steatosis in the liver [15–17]. However, little is known about the connection between activated HSCs and IR injury in SL. Furthermore, there are few studies on the involvement of Rho signaling in the activation of HSCs in SL.

The aim of the present study was to investigate the association between Rho signaling and the activation of HSCs in SL. We also examined whether inhibition of the Rho/ROCK pathway could ameliorate IR injury in the steatotic rat liver.

Materials and methods

Animals

Four-week-old male Wistar rats were purchased from Charles River Breeding Laboratories (Osaka, Japan). Rats were fed either a choline-deficient diet (Hiroshima Institute for Experimental Animals, Hiroshima, Japan) to encourage the development of SL, or a normal diet, which resulted in the development of a normal liver (NL). All animal experiments were performed according to the guidelines set by the US National Institutes of Health (1996).

Liver IR

Under anesthesia, whole rat livers were subjected to warm ischemia by clamping the hepatic artery and portal vein with microvascular clips. The specific ROCK inhibitor fasudil hydrochloride hydrate (fasudil; kindly donated by Asahi Kasei Co., Tokyo, Japan) was used to investigate the effect of ROCK inhibition on liver IR injury. Selected rats were pretreated with 10 mg/kg fasudil (intraperitoneal injection) 30 min before the induction of ischemia.

Isolation of HSCs

HSCs were isolated from rat livers according to previously described procedures [9,18]. Purity was estimated by ordinal light and fluorescence microscopic examination and by indirect enzyme immunoreactivity with an antidesmin antibody (Dako, Versailles, France). HSCs were grown in standard tissue culture plastic flasks in Dulbecco's minimum essential medium with 10% fetal bovine serum and antibiotics.

Collagen gel contraction assay

The contractility of the HSCs was evaluated using hydrated collagen gel lattices on 24-well culture plates as described previously with some modifications [9,19]. To investigate the influence of nitric oxide (NO) on HSCs, the NO synthase inhibitor *N*-nitro-L-arginine methyl ester (L-NAME; Cayman Chemical, Ann Arbor, MI) was used.

Western blot analysis

Primary rat HSCs were left untreated or were treated with 10 μM fasudil and/or 5 nM endothelin-1 (ET-1; Sigma–Aldrich Inc., Tokyo, Japan) for 30 min before homogenization in lysis buffer (Cell Lysis Buffer; Cell Signaling Technology, Danvers, MA). Western blot analysis was performed according to previously described procedures with some modifications [20]. Specific antibodies against β-actin were from Abcam (Tokyo, Japan); those against MLC were from Sigma–Aldrich Inc., and those against P-MLC, cofilin, phosphorylated cofilin (P-Cofilin), and Rho-kinase 2(ROCK2) were from Cell Signaling Technology. The protein expression of ROCK2 was normalized to the level of β-actin. The phosphorylation levels were normalized to the levels of total MLC or cofilin protein expression.

Biochemical assessment

Blood samples were collected from the inferior vena cava. Serum ET-1 concentrations were measured using an Endothelin-1 EIA kit (Phoenix Pharmaceuticals, Inc., Burlingame, CA) according to the manufacturer's instructions. Aspartate aminotransferase (AST) and alanine aminotransferase (ALT) levels were assayed by standard enzymatic methods.

Measurement of portal perfusion pressure in the isolated rat liver

Portal pressure in isolated perfused rat livers was measured according to previously described procedures, with some modifications [21]. The perfusion with Krebs–Henseleit buffer (Sigma–Aldrich Inc.) was continued until the monitored inlet pressure value became stable at a constant flow rate of 0.3 ml min^{-1} liver volume $^{-1}$ (ml).

Confocal immunofluorescence and histological study

Phalloidin staining of isolated HSCs and liver sections was performed according to previously described procedures [22]. Samples were observed under a conventional fluorescence microscope or a laser confocal microscope. For the histological study, liver specimens were collected from the middle hepatic lobe after IR. Formalin-fixed liver tissue sections were stained with hematoxylin and eosin (H&E) and examined microscopically. To assess the activity of HSCs in liver sections, phalloidin staining was performed. To assess the grade of the steatosis, sections were stained for oil red O. Furthermore, the detection of apoptosis in liver tissue sections was achieved by TdT-mediated dUTP-digoxigenin nick-end labeling (TUNEL) staining as previously reported [23].

Statistical analysis

Survival rates were compared using the Kaplan–Meier method and analyzed by the log-rank test. Other data are expressed as average values (SD). Statistical analysis among experimental groups was performed using the *t*-test. *p* values less than 0.05 were considered statistically significant. Statistical analyses were performed using SPSS software, version 16 (SPSS Japan Inc., Tokyo, Japan).

Results

Changes in the morphology of HSCs isolated from steatotic rat livers

At 10 weeks, rats fed a choline-deficient diet developed liver steatosis, characterized by more than 60% of fatty filtration in the hepatocytes with few inflammatory cells and slight fibrosis (Fig. 1A). HSCs isolated from rat SLs (HSCs-SL) showed increased stress fiber formation and F-actin expression compared to HSCs isolated from normal rat livers (HSCs-NL), which were suppressed by fasudil treatment (Fig. 1B). Phalloidin staining of liver sections showed stress fiber formation and F-actin expression around sinusoidal spaces in SL after IR, as well as the suppression of these changes by fasudil (Supplementary Fig. 1).

Contractility of HSCs isolated from normal and steatotic rat livers

To evaluate differences in contractility, HSCs-NL and HSCs-SL were cultured on hydrated collagen gels. Contraction was measured as the reduction in the initial area of the gel. In the absence of vasoactive agents, the areas of the gels with HSCs-SL were

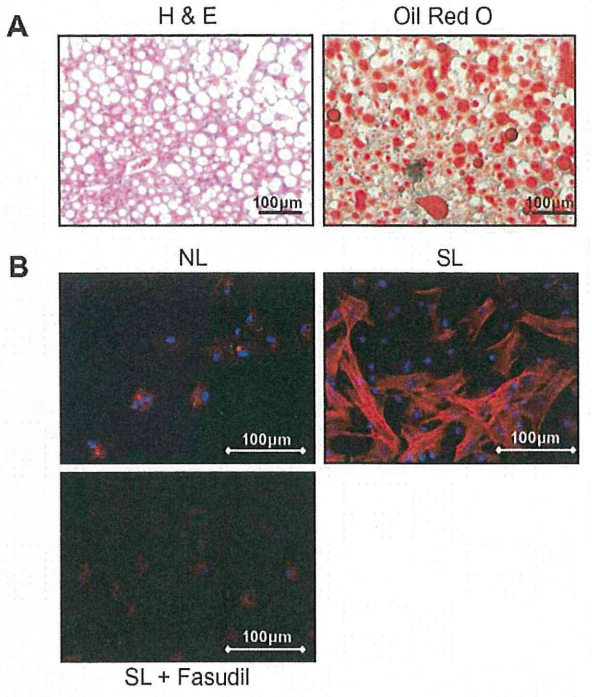

Fig. 1. Oil red O staining and morphology changes of HSCs isolated from rat SL. (A) Representative H&E- and oil red O-stained sections. Rats fed a choline-deficient diet for 6 weeks had more than 60% of macrovesicular steatosis. (B) Images show differences in F-actin expression in isolated HSCs from NL, SL, and SL treated with fasudil (10 μM, 24 h). Cells were stained to show F-actin (red) and nuclei (blue). HSCs isolated from NL showed slight stress fiber formation and F-actin expression. By contrast, HSCs isolated from SL had an elongated, fusiform morphology with prominent dendritic processes. Fasudil suppressed both stress fiber formation and F-actin expression. (For interpretation of the references to colour in this figure legend, the reader is referred to the web version of this article.)

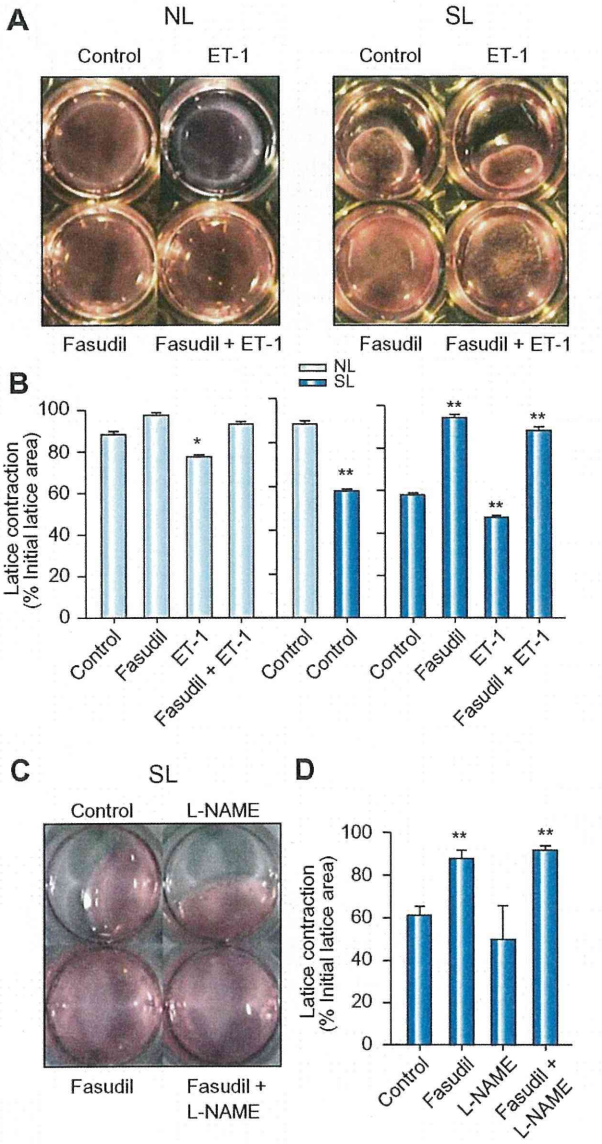

Fig. 2. Collagen gel contraction assay. (A) Contraction of collagen gels induced by the activation of isolated HSCs in untreated NL and SL, and in NL and SL treated with ET-1, fasudil or a combination of the two. Without the addition of HSCs, the collagen gels did not contract during the observation period (not shown). Control, medium alone; ET-1, 5 nM ET-1; Fasudil, 10 μM fasudil; Fasudil + ET-1, 10 μM fasudil and 5 nM ET-1. (C) Contraction of collagen gels in SL and SL treated with L-NAME, fasudil or a combination of the two. Control, medium alone; L-NAME, 100 μM L-NAME; Fasudil, 10 μM fasudil; Fasudil + L-NAME, 10 μM fasudil, and 100 μM L-NAME. (B and D) Changes in the collagen gel area induced by contraction of HSCs. HSCs isolated from rat NL, closed bars; HSCs isolated from rat SL, open bars. Average values (SD) of three independent experiments are shown. *p <0.05 compared to each control; **p <0.01 compared to each control.

significantly smaller than those with HSCs-NL (p <0.01). In the presence of fasudil (10 μM), this reduction in the areas of gels with HSCs-SL was not observed. The gel areas containing HSCs-SL were significantly smaller in the presence of ET-1 (5 nM) than those with HSCs-SL in the absence of ET-1 (p <0.01). In sharp contrast, however, when fasudil was added to the culture medium in the presence of ET-1, the shrinkage of the gels with HSCs-SL was suppressed (p <0.01; Fig. 2A and B). Furthermore, the NO synthase inhibitor L-NAME (100 μM) was used to investigate the influence of NO on HSCs. Fasudil suppressed the contraction of HSCs-SL even in the presence of L-NAME (p <0.01; Fig. 2C and D).

Expression of ROCK2 and phosphorylation of MLC and cofilin

To examine the possible involvement of the Rho/ROCK pathway in the activation of HSCs, the expression of ROCK2 and the phosphorylation state of MLC and cofilin, a downstream effector of Rho/ROCK signaling, were assessed by Western blot analysis with monoclonal antibodies to ROCK2 and the phosphorylated form of MLC and cofilin. Quantitative analysis using a scanning densitometer confirmed that ROCK2 was significantly overexpressed in HSCs-SL compared with HSCs-NL (p <0.01) (Fig. 3A). The phosphorylation level of MLC in HSCs-SL was significantly increased compared with that in HSCs-NL. The phosphorylation levels of MLC and cofilin were significantly enhanced by ET-1 in HSCs-SL

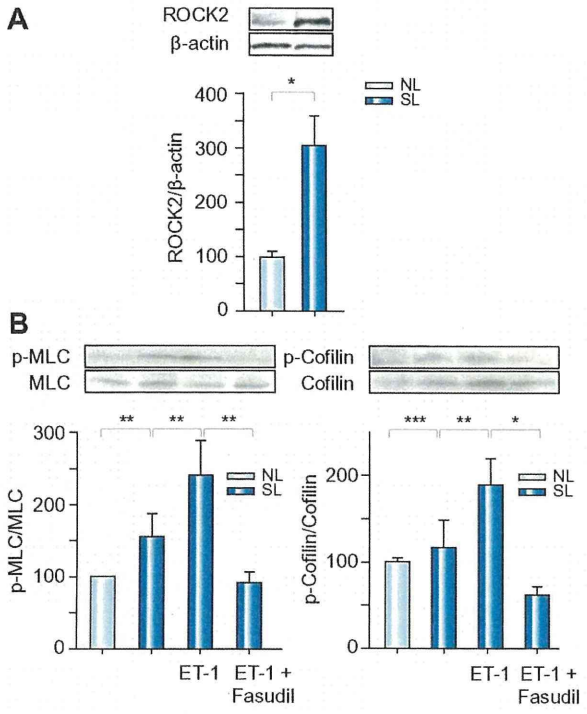

Fig. 3. Western blot analyses in rat HSCs isolated from rat NL or SL. (A) Expression level of ROCK2. (B) Total and phosphorylated MLC and cofilin. HSCs isolated from rat SL were either left untreated or cultured with 10 μM fasudil and/or 5 nM ET-1 for 30 min. The protein expression of ROCK2 was normalized to the level of β-actin. The phosphorylation levels of MLC and cofilin were normalized to total MLC and cofilin protein expression, respectively. Each figure is representative of three independent experiments. Average values (SD) for individual groups are shown. *p <0.01, **p <0.05, ***N.S.

(p <0.05, in both), but the effects were suppressed by fasudil (p <0.05, 0.01, respectively; Fig. 3B).

Influence of IR on the secretion of ET-1

Serum ET-1 concentrations were measured after 30 min of ischemia followed by 3 h of reperfusion using ELISA. Serum ET-1 concentrations significantly increased after IR in rats with NL (p <0.01). Serum ET-1 concentrations after IR were significantly higher in rats with SL than in rats with NL (p <0.01). Furthermore, fasudil significantly suppressed the serum ET-1 concentrations after IR (p <0.01; Fig. 4).

Influence of IR on portal perfusion pressure

To determine the influence of IR on the microvascular blood flow in the hepatic lobule, the portal perfusion pressure was assessed in isolated rat livers. Perfusion pressures were measured after 45 min of ischemia followed by 15 min of reperfusion. The portal perfusion pressures in rats with SL were significantly higher than those in rats with NL (p <0.05). The portal perfusion pressures in rats with SL after IR were significantly higher than those in rats with SL that did not undergo IR (p <0.01), and the effect was suppressed by fasudil (p <0.01; Fig. 5).

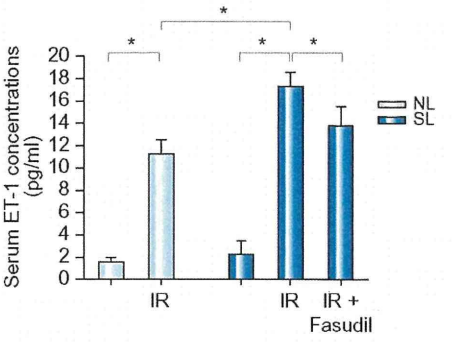

Fig. 4. Serum ET-1 concentrations, reflecting secretion from SECs and HSCs. Blood samples were collected from rats with NL or SL after 30 min of ischemia followed by 3 h of reperfusion. A group of the SL rats received fasudil (10 mg/kg) 30 min before ischemia. Average values (SD) for individual groups are shown; for all groups, n = 6. *p <0.01.

Biochemical assessment, histological study, and survival rates after IR

AST and ALT are well-established markers of hepatocellular injury after IR. Serum AST and ALT levels were measured after 30 min of ischemia followed by 3 or 24 h of reperfusion. The increase in AST at 3 and 24 h and in ALT at 3 h after IR of the untreated rats with SL was significantly higher than in fasudil-treated rats with SL (Fig. 6A). For histological analysis, liver specimens were obtained after 45 min of ischemia followed by 24 h of reperfusion. Liver specimens from untreated rats with SL after IR showed distortion of architecture, sinusoidal congestion, microthrombus, and extensive areas of coagulative necrosis. In contrast, specimens from the SL group treated with 10 mg/kg fasudil showed almost normal hepatic structure (Fig. 6B). TUNEL staining of liver tissue sections after IR showed that most hepatocytes in NL were TUNEL positive, whereas only minimal TUNEL staining was found in SL (Supplementary Fig. 2). The survival rate of rats with SL that underwent 45 min of ischemia was significantly lower than that of rats with NL (p <0.01). However, treat-

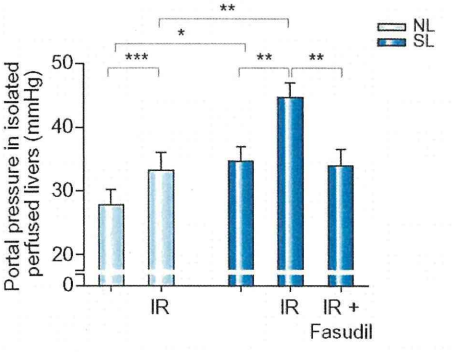

Fig. 5. Portal pressures in isolated perfused livers from rats with NL and SL. Livers were untreated, treated with 45 min of ischemia followed by 15 min of reperfusion, or preinjected with 10 mg/kg fasudil intraperitoneally 30 min before IR. Average values (SD) for individual groups are shown; for all groups, n = 5. *p <0.05; **p <0.01, ***N.S.

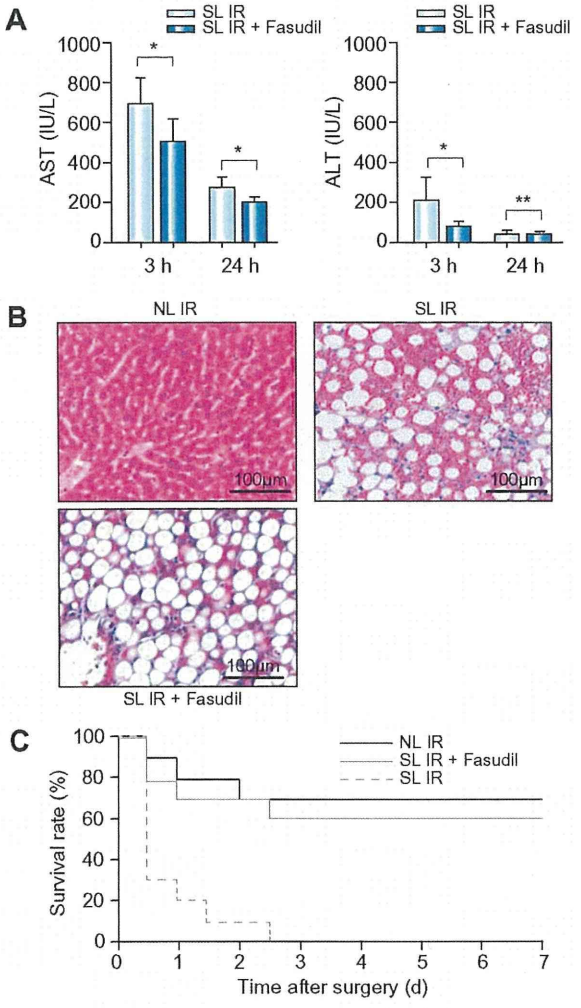

Fig. 6. Influence of IR in rats with SL. Rats with NL or SL were treated with IR. A fraction of the SL group received fasudil (10 mg/kg) 30 min before IR. (A) Serum levels of AST and ALT in rats with SL after 30 min of ischemia followed by 3 and 24 h of reperfusion. Average values (SD) for individual groups are shown; for all groups, n = 5. *p <0.05, **N.S. (B) Histological examination of NL and SL after 45 min of ischemia followed by 24 h of reperfusion. Liver specimens from untreated rats with SL showed severe fat accumulation, distortion of architecture, sinusoidal congestion, and extensive areas of coagulative necrosis. Liver specimens from the group that received fasudil similarly showed severe fat accumulation but had a nearly normal hepatic structure and minimal sinusoidal enlargement in the hepatic lobule center compared with the untreated SL. Representative H&E-stained liver sections. (C) The survival rates of rats with NL or SL that underwent 45 min of ischemia. Although the survival rate of the SL group was significantly lower than that of the NL group (p <0.01), fasudil treatment significantly improved the survival rate of the SL group (p <0.01), n = 10.

ment with fasudil significantly improved the survival rate of rats with SL after IR (p <0.01; Fig. 6C).

Discussion

The SL is known to be vulnerable to IR compared with the NL. The present study is the first report to provide evidence of the effect of Rho/ROCK signaling activation in HSCs on the increased susceptibility of SL to IR injury in rats. The present results showed that the activation of HSCs in SL was associated with the upregulation of ROCK2 and that the enhanced activation of ROCK2 was involved in the induction of IR injury in SL. The intra-abdominal infusion of fasudil, a specific inhibitor of ROCK, significantly alleviated IR injury in SL.

ROCK is a downstream effector of the small GTPase Rho involved in the regulation of cytoskeletal rearrangements and cell migration. ROCK is involved in the contraction of activated HSCs, which play an important role in regulating hepatic microcirculation. Intrahepatic upregulation of ROCK contributes to increased intrahepatic resistance in cirrhotic rats and to an increased sensitivity of cirrhotic livers to vasoconstrictors [24].

In the current study, HSCs-SL showed greater stress fiber formation and overexpression of ROCK compared with NL. The contractility of the HSCs and the phosphorylation of MLC in the HSCs were significantly enhanced in SL compared with NL. These results indicated a significant activation of the HSCs-SL compared with the HSCs-NL. There have been few studies using HSCs-SL. However, liver biopsy specimens from SL and nonalcoholic steatohepatitis showed the presence of activated HSCs, identified immunohistologically using a specific monoclonal antibody to detect cytoplasmic α-smooth muscle actin, which is not present in quiescent cells. These findings revealed a correlation between the degree of HSC activation and hepatic fibrosis, and the study of these specimens suggested a trend toward increased HSC activation with increasing fat accumulation, although this lacked statistical significance [15–17]. The hepatic expression of ROCK has been shown to be elevated in livers from cirrhotic rats and patients with alcohol-induced cirrhosis, and intrahepatic upregulation of ROCK contributes to portal hypertension via an increase in hepatic vascular resistance [24]. These results indicate that the activation of HSCs may be related to the overexpression of ROCK.

In our previous report using normal rat livers, the IR-induced impairment of sinusoidal microcirculation resulted, in part, from the contraction of HSCs, and Y-27632, a specific ROCK inhibitor, suppressed the IR-induced microcirculatory disturbance by promoting the relaxation of HSCs [9].

In the present study, the portal perfusion pressure was significantly increased in SL compared with NL. The perfusion pressure in SL was further increased after IR, and fasudil significantly suppressed this pressure increase. Serum ET-1 concentration was also significantly elevated after IR, and the increase in ET-1 concentration was suppressed by the administration of fasudil. These findings indicate that fasudil attenuates microvascular injury following ischemia reperfusion in SL. ET-1, which activates the Rho/ROCK pathway and elevates portal pressure via contraction of HSCs, was used as an alternative marker for IR injury in our *in vitro* studies (including a collagen gel contraction assay and measurement of MLC and cofilin phosphorylation in HSCs). This was done because it was extremely difficult to isolate HSCs from rats with SL undergoing IR owing to insufficient perfusion of pronase and collagenase, and even when successful, the isolated HSCs showed very low viability for use in further *in vitro* studies.

The contractility of the HSCs and the phosphorylation of MLC and cofilin were significantly enhanced by ET-1 in the HSCs-SL, and fasudil attenuated these effects. Furthermore, fasudil prolonged the survival of rats with SL undergoing IR and attenuated

sinusoidal congestion and hepatocyte necrosis. These results indicate that fasudil, a specific ROCK inhibitor, suppresses IR-induced liver injury by ameliorating the hemodynamic disturbance through the modulation of Rho signaling in SL, which is more vulnerable to IR than NL.

Fasudil was used as a ROCK inhibitor in the present study based on the clinical application of the inhibitor for the release of cerebral vasospasm after subarachnoid hemorrhage [25]. Fasudil was administered at a dose of 10 mg/kg by intraperitoneal injection before IR because the area under the serum fasudil concentration curve for rats after the intraperitoneal injection of the inhibitor (10 mg/kg) was 4490 ng h/ml, which was almost compatible or slightly higher than that of fasudil in humans [26]. The use of fasudil may be a new therapeutic strategy to prevent hepatic IR injury.

The results of the current study indicated that the effect of fasudil on the contractility of HSCs-SL was mediated by the direct inhibition of ROCK, and independent of the NO effect in HSCs. Anegawa *et al.* reported that in a rat model of secondary biliary cirrhosis bile duct ligation, ROCK activation with resultant eNOS activation was substantially involved in the pathogenesis of portal hypertension. Moreover, fasudil significantly suppressed ROCK activity and increased eNOS phosphorylation through a reduction of the binding of serine/threonine Akt to ROCK and an increase of the binding of Akt to eNOS [27]. The improvement of hepatic hemodynamics by fasudil has been shown to be mediated by an enhancement of NO production by sinusoidal endothelial cells (SECs), rather than by direct inhibition of Rho-kinase in HSCs. Our result was not compatible with Anegawa's report. This may be due to differences in the experimental model used. We used a collagen gel contraction assay to show that the effect of fasudil on the contractility of HSCs-SL was mediated by direct inhibition of ROCK, while in the study by Anegawa *et al.*, a bile duct ligation-induced secondary biliary cirrhosis model revealed that the hemodynamic effects of the *in vivo* administration of fasudil were associated with the production of NO by SECs, and not by direct inhibition of ROCK. The relationship between SL and NO synthesis remains to be elucidated, and further investigation is necessary. In addition, ROCK inhibitors have been reported to improve the VLDL transport functions of hepatocytes in SL, which might be one of the mechanisms underlying their protective effect against IR injury [28].

In summary, activation of Rho/ROCK signaling in HSCs-SL is associated with an increased susceptibility to IR injury. Inhibition of ROCK attenuates the activation of the HSCs-SL and improves IR injury in rats with liver steatosis.

Acknowledgments

The authors thank Asahi Kasei Co., Tokyo, Japan, for providing fasudil. This work was supported in part by a Grant-in-Aid for Scientific Research (KAKENHI 21591748 [to H.T.]) from the Ministry of Education, Science, Sports, and Culture of Japan.

Conflict of interest

The authors who have taken part in this study declared that they do not have anything to disclose regarding funding or conflict of interest with respect to this manuscript.

Supplementary data

Supplementary data associated with this article can be found, in the online version, at doi:10.1016/j.jhep.2011.04.029.

References

[1] McCormack L, Petrowsky H, Jochum W, Furrer K, Clavien PA. Hepatic steatosis is a risk factor for postoperative complications after major hepatectomy: a matched case-control study. Ann Surg 2007;245:923–930.
[2] Gomez D, Malik HZ, Bonney GK, Wong V, Toogood GJ, Lodge JP, et al. Steatosis predicts postoperative morbidity following hepatic resection for colorectal metastasis. Br J Surg 2007;94:1395–1402.
[3] Trevisani F, Colantoni A, Caraceni P, Van Thiel DH. The use of donor fatty liver for liver transplantation: a challenge or a quagmire? J Hepatol 1996;24:114–121.
[4] Hui AM, Kawasaki S, Makuuchi M, Nakayama J, Ikegami T, Miyagawa S. Liver injury following normothermic ischemia in steatotic rat liver. Hepatology 1994;20:1287–1293.
[5] Wada K, Fujimoto K, Fujikawa Y, Shibayama Y, Mitsui H, Nakata K. Sinusoidal stenosis as the cause of portal hypertension in choline deficient diet induced fatty cirrhosis of the rat liver. Acta Pathol Jpn 1974;24:207–217.
[6] Caraceni P, Ryu HS, Subbotin V, De Maria N, Colantoni A, Roberts L, et al. Rat hepatocytes isolated from alcohol-induced fatty liver have an increased sensitivity to anoxic injury. Hepatology 1997;25:943–949.
[7] Seifalian AM, Chidambaram V, Rolles K, Davidson BR. In vivo demonstration of impaired microcirculation in steatotic human liver grafts. Liver Transpl Surg 1998;4:71–77.
[8] Zhang JX, Bauer M, Clemens MG. Vessel- and target cell-specific actions of endothelin-1 and endothelin-3 in rat liver. Am J Physiol 1995;269.
[9] Mizunuma K, Ohdan H, Tashiro H, Fudaba Y, Ito H, Asahara T. Prevention of ischemia-reperfusion-induced hepatic microcirculatory disruption by inhibiting stellate cell contraction using rock inhibitor. Transplantation 2003;75:579–586.
[10] Ankoma-Sey V, Wang Y, Dai Z. Hypoxic stimulation of vascular endothelial growth factor expression in activated rat hepatic stellate cells. Hepatology 2000;31:141–148.
[11] Hirose M, Ishizaki T, Watanabe N, Uehata M, Kranenburg O, Moolenaar WH, et al. Molecular dissection of the Rho-associated protein kinase (p160ROCK)-regulated neurite remodeling in neuroblastoma N1E–115 cells. J Cell Biol 1998;141:1625–1636.
[12] Maekawa M, Ishizaki T, Boku S, Watanabe N, Fujita A, Iwamatsu A, et al. Signaling from Rho to the actin cytoskeleton through protein kinases ROCK and LIM-kinase. Science 1999;285:895–898.
[13] Kimura K, Ito M, Amano M, Chihara K, Fukata Y, Nakafuku M, et al. Regulation of myosin phosphatase by Rho and Rho-associated kinase (Rho-kinase). Science 1996;273:245–248.
[14] Amano M, Chihara K, Kimura K, Fukata Y, Nakamura N, Matsuura Y, et al. Formation of actin stress fibers and focal adhesions enhanced by Rho-kinase. Science 1997;275:1308–1311.
[15] DeLeve LD, Wang X, Kanel GC, Atkinson RD, McCuskey RS. Prevention of hepatic fibrosis in a murine model of metabolic syndrome with nonalcoholic steatohepatitis. Am J Pathol 2008;173:993–1001.
[16] Washington K, Wright K, Shyr Y, Hunter EB, Olson S, Raiford DS. Hepatic stellate cell activation in nonalcoholic steatohepatitis and fatty liver. Hum Pathol 2000;31:822–828.
[17] Reeves HL, Burt AD, Wood S, Day CP. Hepatic stellate cell activation occurs in the absence of hepatitis in alcoholic liver disease and correlates with the severity of steatosis. J Hepatol 1996;25:677–683.
[18] Elinav E, Ali M, Bruck R, Brazowski E, Phillips A, Shapira Y, et al. Competitive inhibition of leptin signaling results in amelioration of liver fibrosis through modulation of stellate cell function. Hepatology 2009;49:278–286.
[19] Sohail MA, Hashmi AZ, Hakim W, Watanabe A, Zipprich A, Groszmann RJ, et al. Adenosine induces loss of actin stress fibers and inhibits contraction in hepatic stellate cells via Rho inhibition. Hepatology 2009;49:185–194.
[20] Ushitora Y, Tashiro H, Ogawa T, Tanimoto Y, Kuroda S, Kobayashi T, et al. Suppression of hepatocellular carcinoma recurrence after rat liver transplantation by FTY720, a sphingosine-1-phosphate analog. Transplantation 2009;88:980–986.
[21] Ikeda H, Nagashima K, Yanase M, Tomiya T, Arai M, Inoue Y, et al. Sphingosine 1-phosphate enhances portal pressure in isolated perfused liver via S1P2 with Rho activation. Biochem Biophys Res Commun 2004;320:754–759.

[22] van der Heijden M, Versteilen AM, Sipkema P, van Nieuw Amerongen GP, Musters RJ, Groeneveld AB. Rho-kinase-dependent F-actin rearrangement is involved in the inhibition of PI3-kinase/Akt during ischemia-reperfusion-induced endothelial cell apoptosis. Apoptosis 2008;13:404–412.
[23] Selzner M, Rudiger HA, Sindram D, Madden J, Clavien PA. Mechanisms of ischemic injury are different in the steatotic and normal rat liver. Hepatology 2000;32:1280–1288.
[24] Zhou Q, Hennenberg M, Trebicka J, Jochem K, Leifeld L, Biecker E, et al. Intrahepatic upregulation of RhoA and Rho-kinase signalling contributes to increased hepatic vascular resistance in rats with secondary biliary cirrhosis. Gut 2006;55:1296–1305.
[25] Suzuki Y, Shibuya M, Satoh S, Sugimoto Y, Takakura K. A postmarketing surveillance study of fasudil treatment after aneurysmal subarachnoid hemorrhage. Surg Neurol 2007;68:126–131.
[26] Satoh S, Utsunomiya T, Tsurui K, Kobayashi T, Ikegaki I, Sasaki Y, et al. Pharmacological profile of hydroxy fasudil as a selective rho kinase inhibitor on ischemic brain damage. Life Sci 2001;69:1441–1453.
[27] Anegawa G, Kawanaka H, Yoshida D, Konishi K, Yamaguchi S, Kinjo N, et al. Defective endothelial nitric oxide synthase signaling is mediated by rho-kinase activation in rats with secondary biliary cirrhosis. Hepatology 2008;47:966–977.
[28] Kitamura K, Tada S, Nakamoto N, Toda K, Horikawa H, Kurita S, et al. Rho/Rho kinase is a key enzyme system involved in the angiotensin II signaling pathway of liver fibrosis and steatosis. J Gastroenterol Hepatol 2007;22:2022–2033.

Cell Transplantation, Vol. 20, pp. 1915–1920, 2011
Printed in the USA.

0963-6897/11 $90.00 + .00
DOI: http://dx.doi.org/10.3727/096368911X566253
E-ISSN 1555-3892
www.cognizantcommunication.com

Brief Communication

Human CD47 Expression Permits Survival of Porcine Cells in Immunodeficient Mice That Express SIRPα Capable of Binding to Human CD47

Chunfeng Wang,*†[1] Hui Wang,†‡[1] Kentaro Ide,§ Yuantao Wang,†
Nico Van Rooijen,¶ Hideki Ohdan,§ and Yong-Guang Yang†‡

*College of Animal Science and Technology, Jilin Agricultural University, Changchun, China
†Transplantation Biology Research Center, Massachusetts General Hospital, Harvard Medical School, Boston, MA, USA
‡Columbia Center for Translational Immunology, Columbia University College of Physicians and Surgeons, New York, NY, USA
§Department of Surgery, Division of Frontier Medical Science, Programs for Biomedical Research, Graduate School of Biomedical Science, Hiroshima University, Hiroshima, Japan
¶Department of Cell Biology, Vrije Universiteit, Amsterdam, The Netherlands

Signal regulatory protein α (SIRPα) is a critical immune inhibitory receptor on macrophages, and its interaction with CD47 prevents autologous phagocytosis. We have previously shown that pig CD47 does not interact with human SIRPα, and that human CD47 expression inhibits phagocytosis of porcine cells by human macrophages in vitro. In this study, we have investigated the potential of human CD47 expression to promote porcine cell survival in vivo. Human CD47-expressing and control porcine B-lymphoma cells were transplanted into T- and B-cell-deficient nonobese diabetic/severe combined immunodeficient (NOD/SCID) mice that express SIRPα capable of interacting with human CD47. Only the human CD47-expressing porcine lymphoma cells survived and were able to form tumors in NOD/SCID mice; however, both the control and human CD47-expressing porcine cells survived in macrophage-depleted NOD/SCID mice. These results indicate that transgenic expression of human CD47 may provide an effective approach to inhibiting macrophage-mediated xenograft rejection in clinical xenotransplantation.

Key words: CD47; Macrophage; Pig; Signal regulatory protein α (SIRPα); Xenotransplantation

INTRODUCTION

Xenotransplantation from pigs may provide a solution to the scarcity of human donors, but this type of clinical translation is primarily hampered by strong xenoimmune responses (7,16,20,28). Because of the extensive molecular incompatibilities between the donor and host, innate immune responses, including those mediated by natural antibodies, complement, macrophages, and natural killer (NK) cells, play a much greater role in the rejection of xenografts than in allograft rejection. Recipient macrophages are activated and rapidly recruited after xenotransplantation, and their responses to xenoantigens occur before T-cell activation (10). Macrophages cause almost immediate rejection of xenogeneic bone marrow cells, even in the absence of adaptive immunity (1,3), which poses a formidable obstacle to the application of mixed chimerism for induction of xenotransplantation tolerance. Macrophages have also been found to mediate the rejection of porcine islet xenografts in both rodents (9,11,17,26) and primates (19).

Macrophage activation is regulated by the balance between stimulatory and inhibitory signals. CD47 (also known as the integrin-associated protein) is a member

Received September 23, 2010; final acceptance February 15, 2011. Online prepub date: April 29, 2011.
[1]These authors provided equal contribution to this work.
Address correspondence to Yong-Guang Yang, M.D., Ph.D., Columbia Center for Translational Immunology, Columbia University College of Physicians and Surgeons, 630 West 168th St, PS17-514, New York, NY 10032, USA. Tel: (212) 304-5586; Fax: (646) 426-0036;
E-mail: yy2324@columbia.edu

of the Ig superfamily and it is expressed ubiquitously in all tissues (5). Signaling regulatory protein α (SIRPα) (also known as CD172a or SHPS-1) is an inhibitory receptor expressed on macrophages and dendritic cells (DCs) that recognizes CD47 as a "marker of self" (2,5). The CD47–SIRPα interaction provides a "don't eat me" signal to macrophages, which is required for preventing phagocytosis of normal self-hematopoietic cells. We have recently shown that the lack of interaction between pig CD47 and mouse SIRPα is critically associated with macrophage-mediated xenograft rejection in mice (24). We also observed that pig CD47 does not functionally interact with human SIRPα, and that human CD47 expression reduces phagocytosis of porcine cells by human macrophages in vitro (12). A recent study demonstrated that, due to polymorphisms in the nonobese diabetic (NOD) SIRPα allele, NOD mouse SIRPα is capable of cross-reacting with human CD47, and such cross-reactivity prevents human hematopoietic cells from rejection by macrophages in the mouse model (21). In the present study, we used NOD/SCID (severe combined immunodeficient) mice to assess the potential of human CD47 expression to inhibit macrophage-mediated rejection of porcine cells in vivo.

MATERIALS AND METHODS

Mice and Cell Lines

Nonobese diabetic/severe combined immunodeficient (NOD/SCID) mice were purchased from The Jackson Laboratory (Bar Harbor, ME), and housed in a specific pathogen-free microisolator environment. Protocols involving animals used in this study were approved by the Massachusetts General Hospital Subcommittee of Research Animal Care, and all of the experiments were performed accordingly. Human CD47-expressing (hCD47-LCL) and control (pKS-LCL) porcine cell lines were generated by transfecting porcine B lymphoma cell line (LCL) cells with pKS336-hCD47 or empty pKS336 vector, respectively, as described previously (12).

In Vitro Cytotoxicity Assay

hCD47-LCL cells and pKS-LCL cells were mixed (at 1:1 ratio) and cocultured (4×10^4/well) with or without human macrophages in 24-well plates, and the ratios of hCD47-LCL cells to pKS-LCL cells in the cultures were determined every day for 8 days by flow cytometry using anti-human CD47 mAb (B6H12; Pharmingen, San Diego, CA) and anti-pig major histocompatibility complex class I (pMHC-I; clone 2.27.3). Human macrophages were differentiated from human monocytic leukemia cell line THP-1 cells (ATCC, Manassas, VA) by stimulation with phorbol myristate acetate (100 ng/ml) for 2 days, and were used after washing out the nonadherent cells.

Porcine Cell Transplantation in NOD/SCID Mice

Porcine cells were injected into the peritoneal cavity or renal subcapsular space of NOD/SCID mice. Some NOD/SCID mice were treated with clodronate liposomes to deplete macrophages. Clodronate was a gift from Roche Diagnostics GmbH (Mannheim, Germany), and liposome encapsulation was performed as described previously (22). NOD/SCID mice were intravenously injected with clodronate liposomes every 5 days until analysis. Porcine cell survival was determined by flow cytometric analysis (FACScalibur; BD Biosciences, San Jose, CA) using fluorescence-conjugated anti-pMHC-I (clone 2.27.3) and anti-human CD47 (B6H12). Each experimental group contained between 3 and 12 mice.

Statistical Analysis

Significant differences between groups were determined by Student's *t*-test using Prism 4 (GraphPad Software, San Diego, CA). A value of $p < 0.05$ was considered statistically significant.

RESULTS

Human CD47 Expression Enables Porcine LCL Cells to Survive in NOD/SCID Mice

We first compared the survival of hCD47-LCL and pKS-LCL) porcine LCL cells in NOD/SCID mice after IP injection. In vitro assay confirmed that hCD47-LCL cells are significantly more resistant than pKS-LCL cells to destruction by human macrophages (Fig. 1), which is consistent with our previous observations (12). NOD/SCID mice were injected IP with the 1:1 mixed hCD47-LCL and pKS-LCL cells (5×10^7/mouse in total) (Fig. 2A), and sacrificed either when they first showed signs consistent with tumor development (lethargy, hunched posture, weight loss, and palpable abdominal swelling and/or mass) or at day 45 postinjection. In the 12 mice examined, five developed visible tumors (Fig. 2B). Tumor cell suspensions were subsequently prepared and stained with anti-pig class I and anti-human CD47 in order to detect the survival of hCD47-LCL versus pKS-LCL cells. Flow cytometric analysis of the tumor cell suspensions revealed that all tumor cells from these mice expressed human CD47, indicating that hCD47-LCL, but not pKS-LCL, cells were capable of surviving in NOD/SCID mice (Table 1, Fig. 2B).

Similar results were obtained when a mixture (1:1) of hCD47-LCL and pKS-LCL cells was injected into the renal subcapsular space of NOD/SCID mice. These mice were sacrificed between 2 and 5 weeks after LCL cell injection, and tumors were found in four of the five mice analyzed (Table 1). Again, all surviving tumor cells detected in these mice were determined to be human $CD47^+$ hCD47-LCL cells by flow cytometric analysis

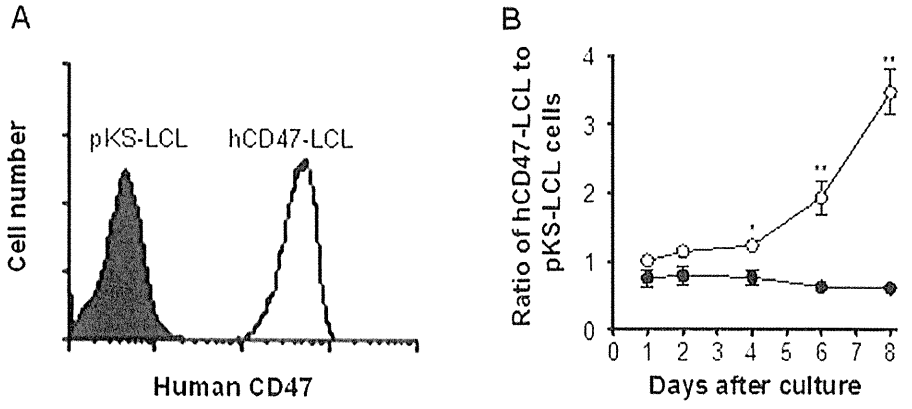

Figure 1. Human CD47 expression reduces the susceptibility porcine lymphoma cell line (LCL) cells to cytotoxicity by human macrophages. hCD47-LCL cells and pKS-LCL cells were mixed (at 1:1 ratio) and cocultured (4×10^4/well) with or without human monocytic leukemia cell line THP-1 macrophages, and the ratios of hCD47-LCL cells to pKS-LCL cells in the cultures were determined every day for 8 days by flow cytometry. (A) Flow cytometric analysis of mixed hCD47-LCL cells and pKS-LCL cells stained with anti-human CD47 mAb (prior to coculture). Open and filled histograms represent hCD47-LCL ($hCD47^+$) and pKS-LCL ($hCD47^-$) cells, respectively. (B) Ratios of hCD47-LCL ($pMHC\text{-}I^+hCD47^+$) to pKS-LCL ($pMHC\text{-}I^+hCD47^-$) cells in the cocultures with (open circles) or without (filled circles) human THP-1 macrophages at the indicated time points. Combined results from three independent experiments are presented. $^*p < 0.01$; $^{**}p < 0.001$.

using anti-human CD47 mAb (Table 1, Fig. 2C, D). These results clearly show that human CD47 expression is capable of markedly improving the survival of porcine LCL cells in NOD/SCID mice.

Recipient Macrophages Are Responsible for the Rejection of Porcine LCL Cells in NOD/SCID Mice

To determine whether the observed advantage of hCD47-LCL cells over pKS-LCL cells to survive in NOD/SCID mice was due to protection against phagocytosis by human CD47 expression, we next compared the survival of these cells in macrophage-depleted NOD/SCID mice. Macrophage depletion was achieved by injection of clodronate liposomes as previously described (1,23). NOD/SCID mice were treated with clodronate liposomes every 5 days; 3 days after the first injection of clodronate liposomes, hCD47-LCL and pKS-LCL cells were injected into the subcapsular space of left and right kidney, respectively. These mice were sacrificed 5 weeks later and all had developed large tumors on both kidneys ($n = 3$) (Fig. 3A, B). Flow cytometric analysis of excised tumor cell suspensions demonstrated that the tumors on the left and right kidneys were formed by the respectively injected hCD47-LCL and pKS-LCL cells (Fig. 3C). Despite the relatively small number of mice examined, this result provides strong evidence that pKS-LCL cells are capable of surviving in macrophage-depleted NOD/SCID mice. Taken together, our data indicate that porcine LCL cells are susceptible to rejection by macrophages, and that human CD47 expression is capable of preventing LCL cells from destruction by macrophages in NOD/SCID mice.

DISCUSSION

In the study presented herein, we show that human CD47-expressing porcine LCL cells can survive as xenografts in NOD/SCID mice. However, both human CD47-expressing and control porcine LCL cells were able to survive in macrophage-depleted NOD/SCID mice, demonstrating that human CD47 expression was able to prevent porcine cells from being rejected via destruction by recipient macrophages. Because NOD/SCID mouse SIRPα is known to be capable of interacting with human CD47 (21), these results indicated that the protective effect of human CD47 expression is likely mediated through a SIRPα-related mechanism providing inhibitory signals to recipient macrophages. Further studies using SIRPα blockades or SIRPα-deficient recipients are needed to draw a conclusion.

We had previously reported that porcine hematopoietic chimerism can be established in triple porcine cytokine [interleukin 3 (IL-3), granulocyte-macrophage colony stimulating factor (GM-CSF), and stem cell factor (SCF)] transgenic NOD/SCID mice after administration of large numbers of porcine bone marrow cells (approximately 1×10^8/mouse) and peripheral blood mononu-

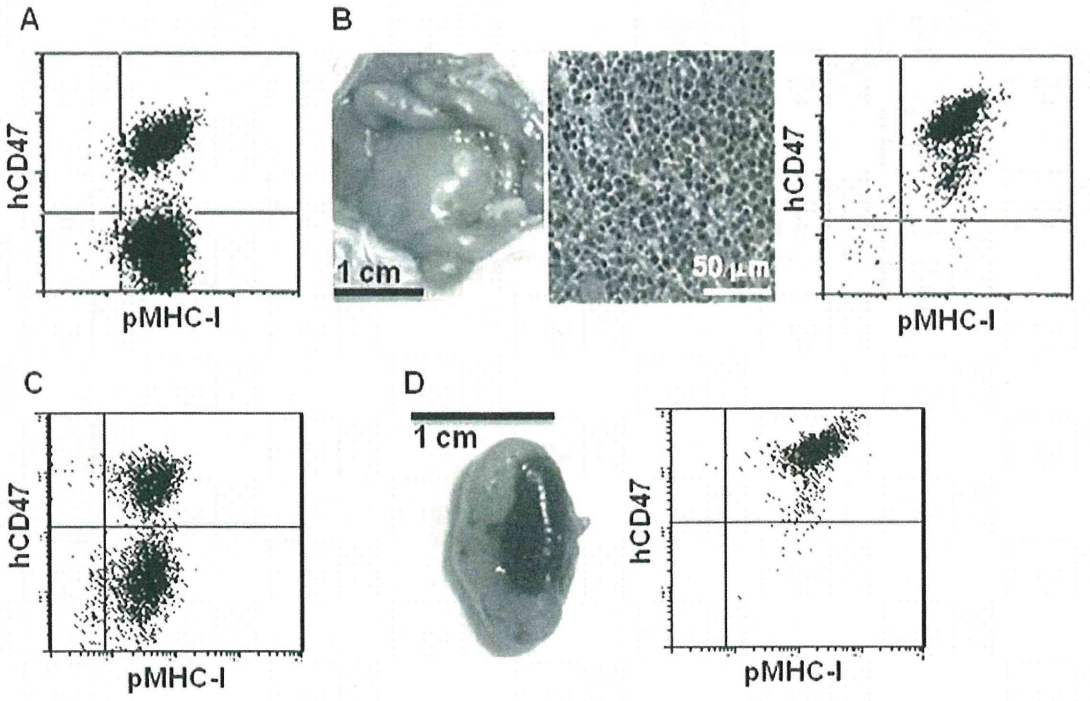

Figure 2. Human CD47-expressing porcine LCL cells show significantly improved survival relative to control LCL cells in NOD/SCID mice. Nonobese diabetic/severe combined immunodeficient (NOD/SCID) mice were injected with 1:1 mixed hCD47-LCL and pKS-LCL cells (5×10^7/mouse in total). (A, B) Porcine cells were injected into the peritoneal cavity of NOD/SCID mice (n = 12; see Table 1). (A) Flow cytometric analysis of the porcine cell inoculum stained with anti-huCD47 and anti-pig major histocompatibility complex (MHC) class I. (B) Macroscopic (left) and histologic (H&E; middle) analysis of tumor tissues, and flow cytometric profile of tumor cell suspension stained with anti-huCD47 and anti-pig MHC class I (right) from a representative mouse. (C, D) Porcine cells were injected into the renal subcapsular space of NOD/SCID mice (n = 5; see Table 1). (C) Porcine cell inoculum stained with anti-huCD47 and anti-pig MHC class I. (D) Macroscopic appearance of a kidney with tumor (left) and flow cytometric analysis of tumor cell suspension (right) from a representative mouse.

clear cells (about 5×10^7/mouse) (6). However, almost all surviving porcine cells in the long-term chimeric mice were found to be CD172a$^+$ myeloid cells. Although the lack of porcine T and B cells in the chimeric mice could possibly be due to the inability of porcine lymphoid cell differentiation to occur in mice, this could also be a consequence of macrophage-mediated rejection, as porcine T and B cells have been shown to survive in macrophage-depleted mice (1). Support for the latter possibility is provided by studies using mouse bone marrow chimeras in which we recently observed that CD47 knock out (KO) macrophage-1 antigen-pos-

Table 1. Tumor Formation by hCD47-LCL and pKS-LCL Cells in NOD/SCID Mice

LCL Cell Administration (n)*	No. With Tumor (Time of Analysis)†	No. With hCD47-LCL/ No. With pKS-LCL‡
Peritoneal cavity (12)	5 (17, 21, 31, 35, 45)	5/0
Kidney capsule (5)	4 (14, 21, 35, 35)	4/0

NOD/SCID, nonobese diabetic/severe combined immunodeficient.
*A mixture (1:1) of hCD47-LCL (human CD47-expressing lymphoma cell line) and pKS-LCL (control porcine LCL) cells (total 5×10^7 cells/mouse) were injected into peritoneal cavity (n = 12) or renal subcapsular space (n = 5).
†Number of mice with visible tumor at sacrifice (days after LCL cell administration).
‡Number of mice with hCD47-LCL (human CD47$^+$) and pKS-LCL (human CD47$^-$) tumor cells determined by flow cytometric analysis of tumor cell suspensions using anti-human CD47 mAb.